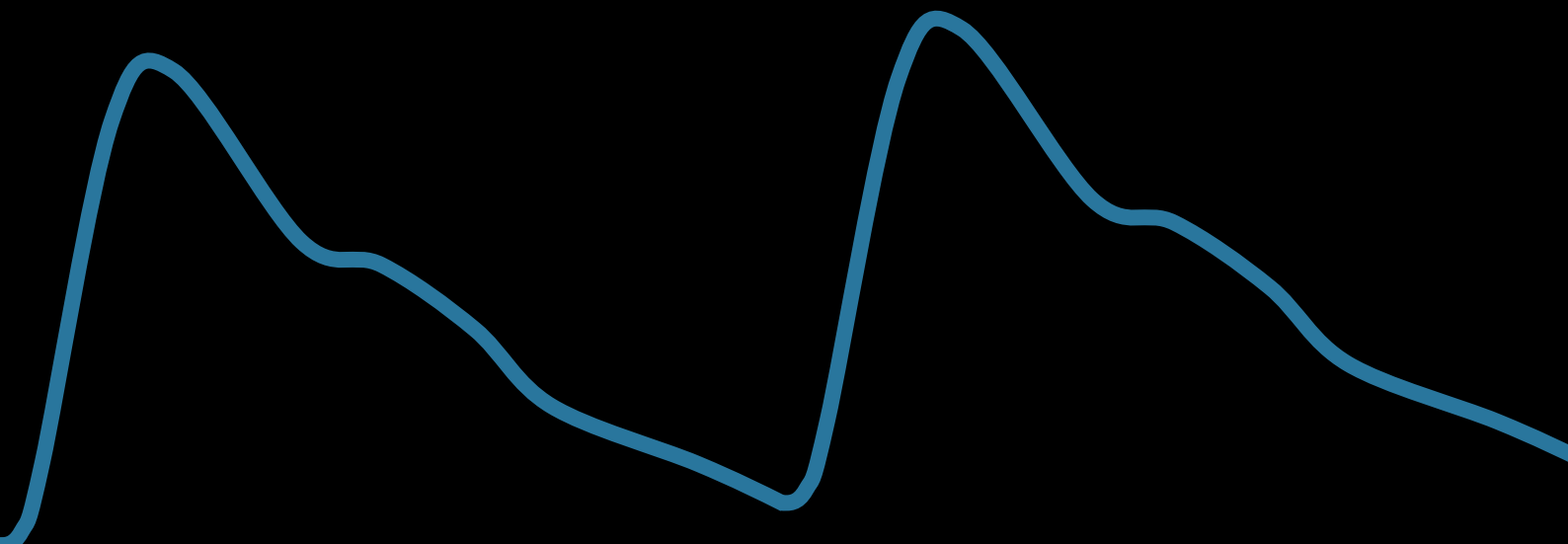


# Characteristics of the wrist-derived photoplethysmography signal: The impact of aortic valve stenosis

Master Thesis  
Technical Medicine



Femke Raijmakers



# Master Thesis

## Technical Medicine

### Characteristics of the wrist-derived photoplethysmography signal: The impact of aortic valve stenosis

**Author:** Femke Raijmakers

**Track:** Medical Sensing and Stimulation

**Educational institution:** University of Twente

**Clinical internship institution:** Cardiology, Radboudumc

Chairman

**Prof. dr. ir. P.H. Veltink**

University of Twente

Biomedical Signals and Systems

Clinical supervisor

**Dr. J. L. Bonnes**

Radboudumc

Cardiology department

Technical supervisor

**Dr. Y. Wang**

University of Twente

Biomedical Signals and Systems

Process supervisor

**Drs. J. de Witte**

University of Twente

Additional supervisor

**R. Edgar MSc**

Radboudumc

Cardiology department

External member

**Dr. ir. A.M. Leferink**

University of Twente

Applied Stem Cell Technologies

10 August, 2023

UNIVERSITY  
OF TWENTE.

Radboudumc



# Abstract

Aortic valve stenosis (AS) is the second most prevalent valvular heart disease in developed countries, and its impact on the healthcare system is expected to increase due to the aging western population. The disease monitoring process of AS using echocardiography imposes high costs and burdens on healthcare professionals and patients. In addition, it remains challenging to anticipate to the unpredictable nature of disease deterioration. Therefore, a noninvasive tool to remotely monitor AS progression could improve disease management and make the follow-up trajectory more efficient. Photoplethysmography (PPG), a technique often used in wearable devices, offers potential as it correlates with various physiological measurements affected by AS. The aim of this study is to investigate the association between AS and the PPG signal.

We conducted an observational, prospective, multicenter study in patients undergoing a transcatheter aortic valve implantation (TAVI). The TAVI procedure offers a valuable clinical situation to unravel the effect of aortic valve obstruction on the characteristics of PPG signals. By comparing the PPG signal characteristics before and after valve implantation in patients with severe AS, it can be explored how resolving the valve obstruction impacts the signal. PPG data were acquired during the TAVI procedure and an algorithm was developed to select 300 consecutive and good-quality cardiac cycles from these data. Subsequently, the PPG signal characteristics of 156 patients were compared before and after valve implantation. The study demonstrated a significant increase after valve placement in the PPG features: systolic amplitude, area under the curve, upstroke, downstroke,  $(b+e)/a$  ratio, and the  $b/a$  ratio. A significant decrease after valve placement was found for the PPG features: crest time,  $e/a$  ratio, notch time, and the pulse width of the PPG signal at different heights. Significant differences after valve implantation suggest that these PPG signal characteristics could be used as potential indicators of AS progression, such as a decreased systolic amplitude or an increased crest time.

An observational, prospective, single-center study was established to overcome the limitations of the TAVI study. The design and rationale of the study were described in Chapter 5. This study focuses on acquiring data during a transthoracic echocardiogram (TTE) to prevent bias introduced by surgical conditions and explore subtle differences in aortic valve function between patients. Patients with and without AS will be equipped with a wristband incorporating a PPG sensor during their TTE examination. The PPG signal characteristics will be compared between patients with AS and patients without AS. Currently, 71 patients have been included, of which 9 with severe AS, 9 with moderate AS, 1 with mild AS, and 4 with a stenotic bicuspid valve. This study contributes to the development of a remote monitoring device for AS that could potentially be used to reduce the number of unnecessary hospital visits and an earlier diagnosis of disease deterioration.

To summarize, the TAVI study showed promising results indicating the potential of PPG in AS monitoring. These findings emphasize the need for further investigation under nonsurgical conditions, with native valves, and interpatient comparisons, which led to the establishment of the DETECT-REMOTE study. The combination of the results of both studies will contribute to a better understanding of the association between AS and the wrist-derived PPG signal and its potential clinical applications.



# List of abbreviations

AC	Alternating current
AR	Aortic valve regurgitation
AS	Aortic valve stenosis
AUC	Area under the curve
AVA	Aortic valve area
BMI	Body mass index
CABG	Coronary artery bypass grafting
CT	Crest time
CW	Continuous wave
DC	Direct current
ECG	Electrocardiogram
EDC	Electronic data capture
EPR	Electronic patient record
GDPR	General data protection regulation
HF	High frequency
HIPAA	Health insurance portability and accountability act
IPA	Inflection point area
IQR	Interquartile range
LED	Light emitting diode
LF	Low frequency
LV	Left ventricle
LVEF	Left ventricular ejection fraction
LVOT	Left ventricle outflow tract
MA	Moving average
PCI	Percutaneous coronary intervention
PG	Pressure gradient
PPG	Photoplethysmography
PW	Pulse width
PWA	Pulse wave amplitude
PWD	Pulse wave duration
SA	Systolic amplitude
SD	Standard deviation

SDR	Systolic-to-diastolic duration ratio
SVR	Systemic vascular resistance
TAVI	Transcatheter aortic valve implantation
TTE	Transthoracic echocardiogram
VTI	Velocity time integral

# Table of contents

<b>Introduction .....</b>	<b>1</b>
1.1 <i>Purpose of the study</i> .....	1
1.2 <i>Thesis outline</i> .....	1
<b>Clinical background .....</b>	<b>3</b>
2.1 <i>Anatomy of the aortic valve</i> .....	3
2.2 <i>Pathology of aortic valve stenosis</i> .....	3
2.3 <i>Diagnosis of aortic valve stenosis</i> .....	3
2.4 <i>Transcatheter aortic valve implantation</i> .....	4
2.4.1 <i>Acute effects of TAVI</i> .....	5
<b>Technical background .....</b>	<b>6</b>
3.1 <i>Principles of photoplethysmography</i> .....	6
3.2 <i>Features of the photoplethysmography signal</i> .....	7
3.3 <i>Principles of transthoracic echocardiography</i> .....	10
<b>First study.....</b>	<b>13</b>
Abstract .....	13
4.1 <i>Introduction</i> .....	14
4.2 <i>Method</i> .....	14
4.2.1 <i>Data collection</i> .....	14
4.2.2 <i>Data visualization and exclusion</i> .....	15
4.2.3 <i>PPG signal preprocessing</i> .....	15
Filtering and removing motion artifacts.....	15
Peak detection algorithm .....	15
Segment selection algorithm.....	17
4.2.4 <i>Feature extraction of PPG signal</i> .....	17
4.2.5 <i>Statistical analysis</i> .....	18
4.3 <i>Results</i> .....	20
4.4 <i>Discussion</i> .....	23
4.4.1 <i>Summary of findings</i> .....	23
4.4.2 <i>Interpretation of results</i> .....	23
4.4.3 <i>Limitations</i> .....	24
4.4.4 <i>Future perspectives</i> .....	25
4.5 <i>Conclusion</i> .....	25
<b>Second study .....</b>	<b>26</b>
Abstract .....	26
5.1 <i>Introduction</i> .....	27
5.2 <i>Study Design</i> .....	27
5.2.1 <i>Aim of the Study</i> .....	27
5.2.2 <i>Hypothesis</i> .....	27

5.2.3 Overview of the study design.....	27
5.2.4 Eligibility criteria for the study .....	27
5.2.5 Data collection and monitoring .....	28
5.2.6 PPG Monitoring Device .....	28
5.2.7 Study parameters.....	28
5.2.8 PPG data analysis .....	28
5.2.9 Statistical considerations .....	29
5.2.10 Sample size calculation .....	29
5.2.11 Study organization .....	30
<b>5.3 Discussion .....</b>	<b>30</b>
5.3.1 Rationale for the intervention .....	30
5.3.2 Rationale for the outcome measures .....	31
5.3.3 Limitations.....	31
5.3.4 Current status .....	31
<b>Conclusion .....</b>	<b>31</b>
<b>Discussion.....</b>	<b>32</b>
6.1 <i>Summary of findings</i> .....	32
6.2 <i>Interpretation of findings</i> .....	32
6.3 <i>Clinical implications</i> .....	33
6.4 <i>Recommendations</i> .....	34
<b>Conclusion .....</b>	<b>35</b>
<b>Contribution of the author .....</b>	<b>36</b>
<b>References.....</b>	<b>37</b>
<b>Appendix A Figures.....</b>	<b>41</b>
<b>Appendix B Tables .....</b>	<b>42</b>



# Introduction

## 1.1 Purpose of the study

Aortic valve stenosis (AS) is the second most prevalent valvular heart disease in the developed world, with a prevalence of 12.4% at age over 75 [1]. Due to the aging western population, the impact of AS on the healthcare system is expected to increase even more in the coming decades. Since there is no effective medical therapy to halt disease progression, patients undergo repeated echocardiographic examinations to monitor AS progression, and follow-up frequency depends on AS severity [2]. The transthoracic echocardiogram (TTE) is the gold standard for determining the stage of AS. This disease monitoring process imposes high costs and burdens on healthcare professionals and patients [3]. Furthermore, it remains challenging to anticipate the unpredictable nature of AS deterioration [4]. Developing a noninvasive tool to detect severe AS or remotely monitor AS progression could improve disease management and make the follow-up trajectory more efficient.

Photoplethysmography (PPG) sensors are frequently used in wearable devices to monitor vital parameters such as heart rate and oxygen saturation and detect cardiac arrhythmias such as atrial fibrillation [5]. PPG is a low-cost and noninvasive technique that captures a waveform representing volumetric variations in the peripheral blood circulation [6]. The PPG waveform holds valuable clinical information as the features of the signal can be correlated with various physiological measurements, such as blood pressure and stroke volume [7, 8]. Furthermore, changes in the morphology of the PPG waveform can be related to atherosclerosis because the peripheral pulse becomes damped, delayed, and diminished with increasing severity of vascular disease [6, 9]. Furthermore, autonomic function can be evaluated with PPG by measuring heart rate variability [10]. AS also affects the above-mentioned hemodynamic parameters. For instance, progression of stenosis can lead to decreased stroke volume, delayed pulse upstroke, and autonomic dysfunction [11].

Given the above, it seems prudent to study the relationship between the PPG signal and AS to develop a remote monitoring tool for AS. This relationship is investigated in two exploratory studies. The first study compared PPG signals pre- and post-transcatheter aortic valve implantation (TAVI). By measuring the PPG signal during TAVI, it can be investigated how resolution of the severe aortic valve obstruction influences the PPG signal within patients. To overcome the limitations of the TAVI study, the DETECT-REMOTE study was set up. This study aims to investigate PPG signal characteristics in relation to the presence, absence, and severity of AS in patients undergoing TTE. The rationale and design of this study will be described in this thesis. The results are not yet available as this is an ongoing trial. When the results of these studies are combined, the first steps towards a remote tool for monitoring the progression of AS can be taken.

## 1.2 Thesis outline

An overview of the thesis outline can be found in Figure 1. In Chapter 1, the purpose of this study is introduced. In Chapter 2, the clinical background of this thesis with respect to AS and TAVI is described. The technical background regarding the PPG signal and TTE is described in Chapter 3. Chapter 4 describes the study of the PPG signals obtained during TAVI. Chapter 5 provides the design and rationale of the DETECT-REMOTE study, which focuses on PPG signals obtained during TTE. Chapter 6 encompasses a general discussion of the results, implications, and recommendations, followed by the general conclusion in Chapter 7.

## Introduction

---

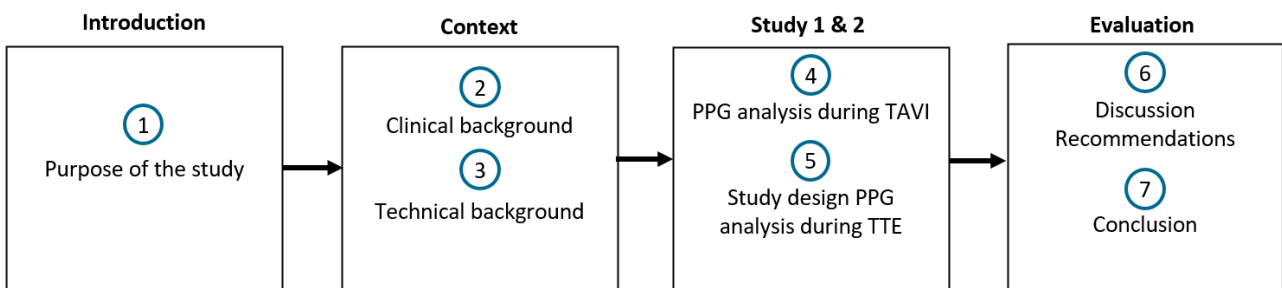


Figure 1: Overview of the thesis structure.

# Clinical background

## 2.1 Anatomy of the aortic valve

The aortic valve is located between the left ventricle (LV) and the aorta to prevent the flow of oxygen-rich blood in the opposite direction. The aortic valve consists of three cusps named after the coronary arteries that arise from the corresponding aortic sinuses: the left coronary cusp, the right coronary cusp, and the non-coronary cusp [12]. An illustration of the aortic valve can be found in Figure 2. The valve divides one of the highest pressure gradients of the cardiopulmonary circuit; hence, it is subject to wear and tear injury [13]. During systole, the pressure in the LV is higher than in the aorta, leading to the opening of the aortic valve and a bloodstream towards the ascending aorta [13]. On the contrary, during diastole, the pressure in the aorta is higher than in the LV. Backflow of blood due to recoil of the elastic aorta during diastole leads to valve closure and filling of the coronary arteries when the myocardium relaxes [12].

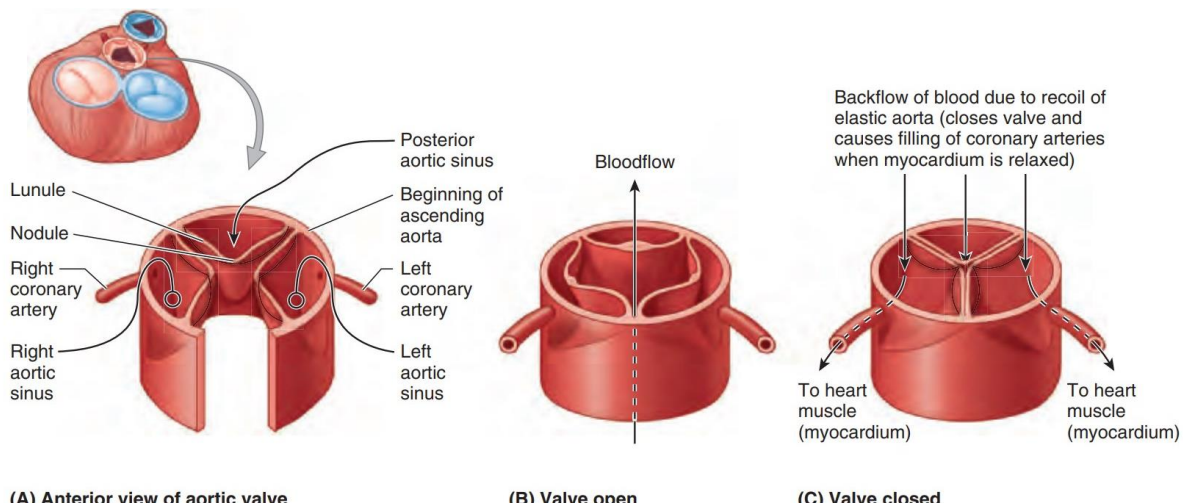


Figure 2: Illustration of the aortic valve, retrieved from [12]. (A) The aortic valve has three semilunar cusps. (B) The ejection of blood from the LV forces the cusps apart. (C) The closing of the valve due to the backflow of blood from the aorta leads to the filling of the coronary arteries.

## 2.2 Pathology of aortic valve stenosis

AS is a cardiovascular condition defined as narrowing of the aortic valve opening, obstructing blood flow from the left ventricle to the ascending aorta during systole. AS is characterized by increased valve stiffness and progressive reduction in valve area, leading to increased left ventricular afterload [14]. An increased afterload can cause left ventricular hypertrophy and a reduced left ventricular ejection fraction (LVEF). Symptoms of severe AS include dyspnea, angina pectoris, syncope, and atrial or ventricular arrhythmia. These symptoms result in poor quality of life and higher hospitalization and mortality rates [14]. The risk of AS increases with age, a bicuspid valve, or a history of rheumatic fever [13, 14]. A bicuspid aortic valve, consisting of two cusps, has a prevalence of 0.7% in male neonates, making it the most common form of congenital heart disease [15].

## 2.3 Diagnosis of aortic valve stenosis

Diagnosis and staging of AS are essential for patient management, risk stratification, and legitimate attribution of symptoms to the valve disease. The clinical exam typically includes the presence of a systolic ejection murmur during auscultation that delays as the disease progresses. This murmur can be heard due

## Clinical background

to the delayed and reduced upstroke of the aortic pressure due to the higher aortic valve pressure gradient [13]. The gold standard for diagnosing and staging AS is TTE with Doppler evaluation [2]. Assessment of AS severity is mainly based on three TTE-derived parameters: the peak velocity over the aortic valve ( $v_{max}$ ), the mean pressure gradient over the aortic valve ( $PG_{mean}$ ), and the aortic valve area (AVA). A more detailed explanation of echocardiography and its parameters can be found in Chapter 2.3. Table 1 provides an overview of the AS staging criteria. In the last decade, this simple and straightforward classification has become a topic of debate due to the observation that up to one-third of patients show a discordant AS grading [2]. Discordant grading occurs when one parameter indicates moderate AS, while the other indicates severe AS.

Table 1: Aortic valve stenosis (AS) grading according to the European Society of Cardiology using echocardiography parameters.  
Mean gradient = mean pressure gradient over the aortic valve, AVA = aortic valve area

Echo parameters	Mild AS	Moderate AS	Severe AS
Peak velocity (m/sec)	2.5 – 3	3 – 4	>4
Mean gradient (mmHg)	<20	20 – 40	>40
AVA (cm <sup>2</sup> )	≥1.5	1 – 1.5	<1

The European Society of Cardiology elaborated this three-parameter method, taking additional parameters into account, such as functional status, stroke volume, Doppler velocity index, LV function, absence or presence of LV hypertrophy, degree of valve calcification, flow conditions, and the adequacy of BP control [2]. The elaborated assessment workflow can be found in Appendix A.1.

## 2.4 Transcatheter aortic valve implantation

TAVI is a procedure in which an arterial catheter is used to guide and fix a biological prosthetic valve at the site of the stenotic aortic valve; see Figure 3. This self-expanding valve is made of memory metal and porcine pericard [15]. The cusps of the stenotic aortic valve will be pressed against the aortic wall by the new valve. Therefore, this procedure can only be performed in patients with a tricuspid valve, meaning the valve consists of three separate valve cusps. Patients with a bicuspid valve are not eligible for this procedure. The most common approach for catheter insertion is through the femoral artery. Alternative routes of catheter incision are through the subclavian artery or through the apex of the heart.

During TAVI procedures, a frequently used technique is rapid ventricular pacing (RVP). RVP is performed using a temporary pacing wire that is placed in the right ventricle through femoral vein access [16]. Pacing the heart suddenly at a high frequency (180 – 220 Hz) causes a temporary reduction in left ventricular stroke volume. This prevents excessive left ventricular afterload and myocardial damage during valve placement.

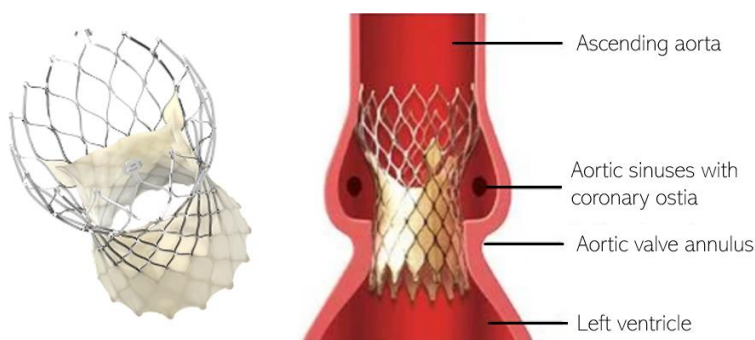


Figure 3: Example of a biological aortic valve and its position after a TAVI procedure. The valve is the Medtronic Evolut R system.  
This illustration is modified from [17, 18].

### 2.4.1 Acute effects of TAVI

The placement of a new valve during a TAVI procedure is associated with several acute hemodynamic changes. Post-TAVI, an immediate increase in systolic aortic pressure and maximal aortic flow is observed which is reached earlier in systole [19]. Concurrently, the ejection duration decreases after TAVI [19]. Furthermore, it is observed that TAVI results in short- and long-term blood pressure elevations. Increased systolic blood pressure after TAVI is associated with an increase in heart rate and stroke volume, which increases cardiac output. Patients with increased blood pressure after TAVI have been demonstrated to have a significantly better clinical outcome, with fewer adverse events than patients with stable blood pressure [20]. Yotti et al. observed that systemic vascular resistance increases directly after valve implantation [21]. Figure 3 shows the aortic pressure wave of a patient with severe AS before (dashed line) and after (continuous line) TAVI [19].

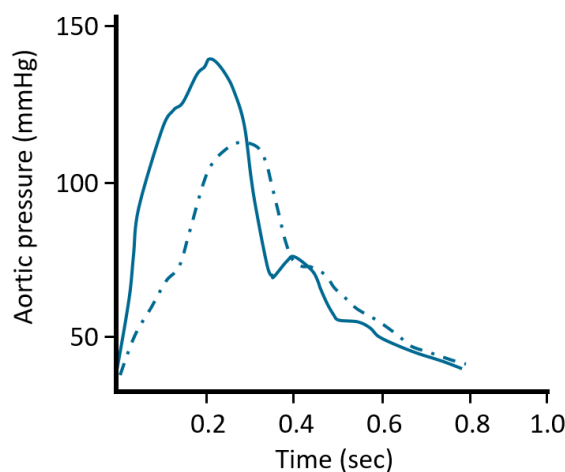


Figure 4: Example of the aortic pressure curve for a patient with severe aortic stenosis before (dashed line) and after (continuous line) TAVI. After TAVI, an increase in the systolic aortic pressure reached earlier can be observed. Furthermore, the slight increase in pressure due to the closure of the aortic valve around 0.4 seconds is more evident after TAVI. The figure is modified from [19].

# Technical background

## 3.1 Principles of photoplethysmography

PPG is a low-cost and noninvasive technique that captures a waveform representing volumetric variations in the peripheral blood circulation [22]. The working principle of PPG is based on the emission of light that penetrates the skin and blood vessels. A photoelectric diode in the PPG sensor detects the amount of light reflected by the tissue. During systole, the blood volume is higher, resulting in an increased amount of light absorption by the tissue and a decreased reflection. Therefore, the PPG sensor measures a lower signal intensity during systole than during diastole. To simplify the interpretation of the signal, the elements of the PPG wave are inverted, so that an increase in waveform amplitude corresponds to an increase in blood volume. Blood volume increases during systole and decreases during diastole, resulting in the PPG waveform in Figure 6.

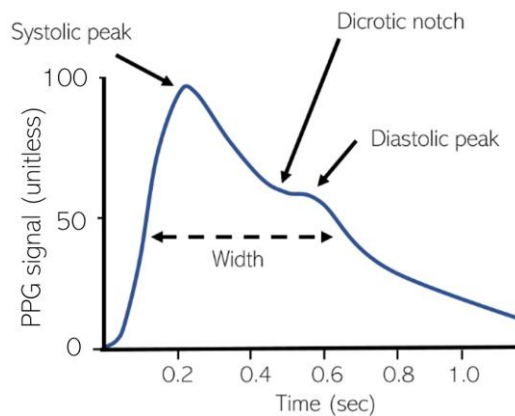


Figure 5: Illustration of a peripherally measured PPG signal during one cardiac cycle with the dicrotic notch intercepting the systolic and diastolic phases.

The PPG signal can be divided into two components: a pulsatile component, called the alternating current (AC), and a low-frequency component, called the direct current (DC). The slowly varying DC component results from the total local blood volume, respiration rate, vasomotor activity, and thermoregulation [22]. The AC component fluctuates with heart rate and can be used to separate the phases of the cardiac cycle and provide information on vasoconstriction and vasodilation [22].

The AC component is similar, though distinct, to the aortic pressure measured invasively in the aorta. In the aortic pressure signal, a notch, known as the incisura, intercepts the systolic and diastolic waveforms. The incisura results from a slight pressure increase due to the aortic valve closure [23]. As PPG signals are acquired noninvasively and peripherally, the incisura diminishes and is replaced by the dicrotic notch, as can be seen in Figure 6. The dicrotic notch arises from a small backflow of blood toward the arterioles when the bloodstream is located at the junction between elastic arteries and inelastic capillaries.

Three different light-emitting diode (LED) colors are often used to obtain PPG waveforms: green, red, and infrared [24]. Red and infrared light can reach a depth of approximately 2.5 mm, whereas green light can reach a depth of less than 1 mm in the tissue. Therefore, the signal obtained by the green light is less prone to artifacts, though less sensitive to small changes in blood volume [22, 24].

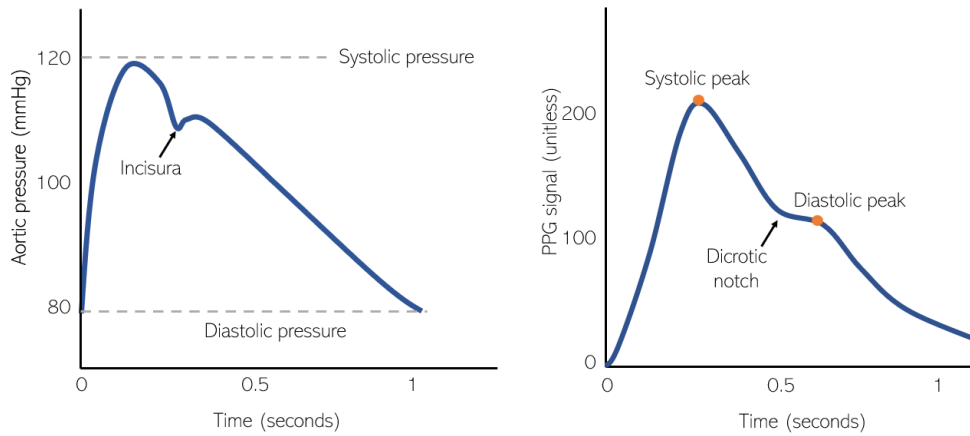


Figure 6: Illustration of the arterial pressure signal (left) and the PPG signal (right) measured during a cardiac cycle. The arterial pressure is measured invasively in the aorta, the PPG signal is measured noninvasively and peripherally at the wrist.

There are two configurations of PPG sensors determined by the location of the light source and the detector [24]. The most commonly used technique is the transmission mode, in which the tissue is placed between the light source and the detector. This configuration is used in the finger pulse oximeter. A disadvantage of this mode is discomfort for daily use, as the common measurement sites are the earlobe and the finger. Therefore, this mode will not be used in this study. The second mode is the reflection mode, where the light source and detector are positioned side by side, and the measurement is based on backscattered light. This mode yields a PPG waveform with a lower amplitude than the transmission mode and is more sensitive to optical shunting, which is the direct detection of light that has not penetrated the tissue. However, the effect of optical shunting can be avoided with appropriate sensor development. Another drawback of the reflection mode is that the sensor is more prone to movement, increasing the risk of motion artifacts [25]. Reflection mode is used in most smartwatches because it can be worn on the wrist, making it user-friendly. This type of PPG sensor is also used in the wristband used in this study.

### 3.2 Features of the photoplethysmography signal

It is essential to extract relevant features to analyze and compare the PPG signal. This section will discuss the features that can be extracted from the signal.

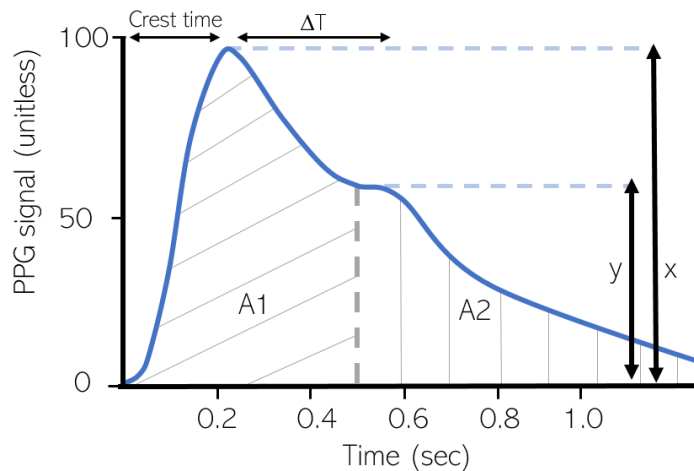


Figure 7: Illustration of a PPG pulse during one cardiac cycle. A1 represents the area under the systolic curve and A2 represents the area under the diastolic curve. X corresponds to the height of the systolic peak, and y corresponds to the height of the diastolic peak. The crest time is the time from the start of the pulse to the systolic peak, and  $\Delta T$  is the time interval between the systolic and diastolic peaks.

### Systolic amplitude

The systolic amplitude is the height of  $x$  in Figure 7. This amplitude varies with changes in the arterial blood flow around the measurement site. This feature has been related to stroke volume and local vascular stiffness [25]. However, this amplitude also depends on external factors such as LED strength, sensor-skin contact surface, scaling, and preprocessing of the signal. Therefore, this parameter only has clinical value in case of a decrease or increase in the same external circumstances.

### Pulse width

The pulse width is the width of the PPG wave, as seen in Figure 5. This width can be determined at different heights of the systolic amplitude. Awad et al. [26] state that the pulse width increases with increased systemic vascular resistance, because the transfer time of the pulse wave lengthens with increased vascular resistance. The transfer time of the pulse wave could also be extended with an increased left ventricular ejection time (LVET). In patients with AS, the LVET could lengthen due to aortic valve obstruction [27].

### Dicrotic notch time

The dicrotic notch is a small notch observed after the peak of the systolic wave in the PPG waveform, marking the end of systole and the beginning of diastole. The dicrotic notch arises from a small backflow of the pulse wave towards the arterioles when the pulse wave is located at the junction between elastic arteries and inelastic capillaries. The dicrotic notch is vaguely related to the behavior of the aortic valve closure [28]. However, it can rather be related to peripheral resistance [23]. The timing of the dicrotic notch depends on the velocity of the pulse wave reflection. A faster pulse wave reflection due to increased vascular stiffness can lead to an earlier occurring notch.

### Augmentation index

The augmentation index is the ratio between  $y$  and  $x$ , as described in Figure 7. This feature provides information on artery compliance [25]. With decreased artery compliance, the backward pulse wave on the junction of the arterioles and capillaries will return faster. This reflected wave will add up to the systolic peak instead of the diastolic peak, decreasing the augmentation index. The augmentation index is not expected to be an indicator of AS on its own, but it can indicate the degree of atherosclerosis that a patient has.

### The area under the curve

The area under the curve (AUC) of the PPG signal represents the amount of pulsatile arterial blood in the measured area over one heartbeat, which can be interpreted as the local stroke volume [25]. Progression of AS can lead to decreased stroke volume that could potentially be measured with the AUC of the PPG signal [2].

### Inflection point area ratio

Systemic vascular resistance can be indicated with the inflection point area ratio (IPA) [25]. The IPA is calculated by the ratio between the AUC of the systolic (A1) and diastolic (A2) peaks, as seen in Figure 8. The IPA is mainly influenced by the pulse wave reflection, resulting from the impedance differences between parts of the arterial system [23]. In patients with severe AS, systemic vascular resistance can be reduced to preserve stroke volume despite reduced left ventricular performance [29].

### Large artery stiffness index

The large artery stiffness index is a person's height divided by the time delay between the systolic and diastolic peaks. This time delay is related to the duration of the pressure wave propagating from the subclavian artery to the peripheral circulation and back to the subclavian artery [25]. The stiffness index increases with age due to the increased stiffness and pulse wave velocity in the aorta and large arteries [25].

### Crest time

The crest time is the time from the onset of the pulse wave to its systolic peak. Alty et al. [30] showed that the crest time is a valuable parameter in predicting the pulse wave velocity, which is an independent predictor of cardiovascular disease. The crest time increases when the vascular resistance increases. The crest time characterizes the early systolic phase, which involves the rapid injection of blood during systole [31].

### Upstroke

The upstroke is the slope from the onset of the pulse wave to the systolic peak. This slope depends on the crest time and the systolic amplitude. A decreased crest time or an increased systolic amplitude will increase the upstroke.

### Downstroke

The downstroke is the slope from the systolic peak to the end of the pulse wave. The downstroke depends on the systolic amplitude and the diastolic duration. These features depend on pulse wave velocity and peripheral blood volume [25].

### Peak-to-peak interval

The peak-to-peak interval is the distance between two consecutive systolic peaks, and it correlates closely to the R-R interval of the electrocardiogram (ECG) [32]. This interval is used to calculate the heart rate and heart rate variability. A study by Blok et al. demonstrates that the heart rate measured with PPG on the wrist with the Cardiowatch from Corsano Health shows an accuracy of 95-98% compared to the heart rate determined by ECG [32]. The Cardiowatch is the wristband that will be used in this study.

### The first and second derivatives

The location of the systolic and diastolic peak and dicrotic notch can be determined by calculating the zeros of the first or second derivatives of the PPG signal. The diastolic peak is located at the index of the third zero of the first derivative, as seen in Figure 8. The dicrotic notch is located at the index of the second zero of the first derivative if there are more than two zeros. If there are less than two zeros, the dicrotic notch can be determined from the *e-wave* of the second derivative, as seen in Figure 8.

The second derivative is used more frequently for analysis than the first [25, 33]. The second derivative consists of four systolic waves and one diastolic wave, as seen in Figure 8. The *a*-, *b*-, *c*-, and *d*-waves are the systolic waves, and the *e-wave* represents the dicrotic notch. The location of the *e-wave* corresponds to the closure of the aortic valve and it is hypothesized that this could provide information on the presence or severity of AS [25].

Commonly derived features from the second derivative are the ratios between the height of each wave and the height of the *a*-wave. For example, the *b/a* ratio increases with age and reflects increased arterial stiffness [28]. Therefore, the *b/a* ratio could be used as a noninvasive indicator of atherosclerosis. The *c/a* ratio and the *e/a* ratio decrease with age and reflect decreased arterial stiffness. The *e/a* ratio can distinguish patients with hypertension from healthy people [23]. The *d/a* ratio reflects decreased arterial stiffness and therefore decreases with age. According to Takazawa et al., the *-d/a* ratio can index left ventricular afterload [34]. The afterload increases with AS and could therefore be a potential marker for AS. The *(b-c-d-e)/a* ratio increases with age and could be helpful in assessing vascular aging. If the *c*- and *d*-waves are missing, one could use the *(b - e)/a* ratio to assess vascular aging [23].

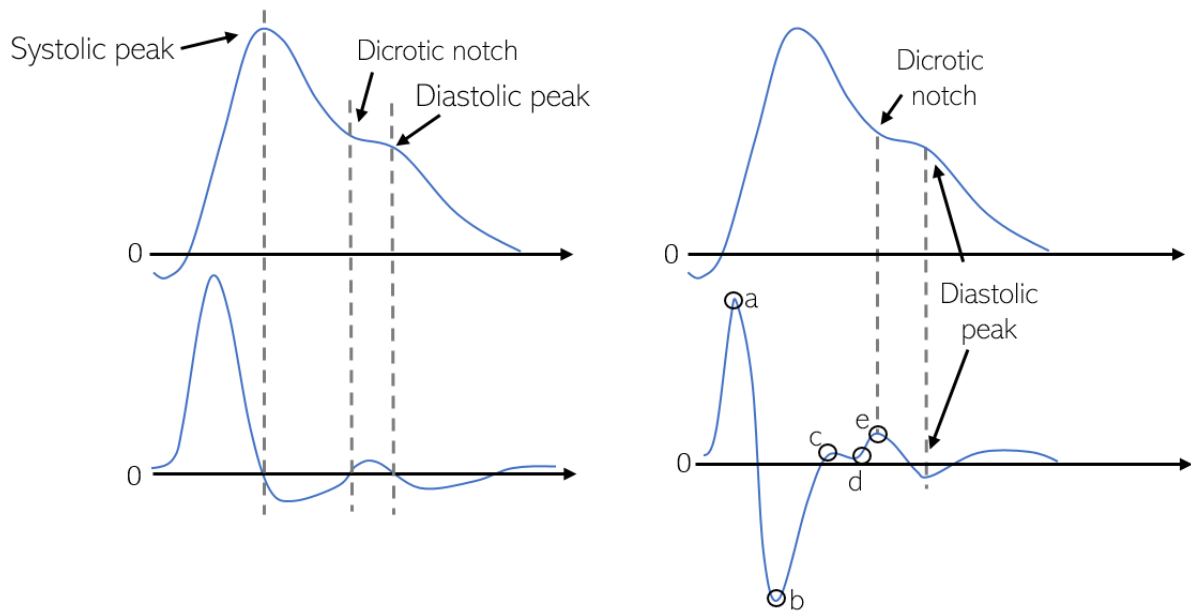


Figure 8: The two graphs on the left show the PPG pulse (top) with its first derivative (bottom). The systolic and diastolic peaks are at the zeros of the first derivative. The PPG pulse and its second derivative can be seen on the right. Three systolic waves (a,b,c,d) and the dicrotic notch (e) can be identified from the second derivative. This figure is modified from [25].

### PPG variability

The PPG variability is defined as the fluctuations in the peak-to-peak interval of the PPG signal. This variable can be represented in the frequency domain, subdivided into low-frequency components (0.04-0.15 Hz) and high-frequency components (0.15-0.4 Hz). Simonyan et al. [10] demonstrated that patients with AS are characterized by a PPG signal with a higher percentage of low-frequency components (%LF) and a higher percentage of high-frequency components (%HF) compared to healthy people. Low-frequency oscillations are associated with sympathetic effects on peripheral vascular resistance, and high-frequency oscillations are associated with respiratory effects [10]. In patients with AS with a decreased LVEF, a compensatory increase in sympathetic activity is observed, which could explain the increased %LF. Simonyan et al. [10] state that an increase in functional activity of the respiratory center could cause an increase in the %HF.

### 3.3 Principles of transthoracic echocardiography

Echocardiography is the gold standard for the initial diagnosis and follow-up of AS. This is a noninvasive imaging technique employing ultrasound waves to assess the structure and function of the heart. Ultrasounds are high-frequency sound waves beyond the audible range [35]. The ultrasound transducer, also called the probe, consists of piezoelectric elements that are able to convert electrical energy to mechanical energy (sound waves) and vice versa. To obtain the ultrasound image, the transducer emits ultrasound waves as a beam towards the heart. This beam travels in a direct line until it encounters a structure with a different acoustical impedance, such as the difference between blood and tissue [35]. This impedance mismatch causes a partial reflection of the ultrasound beam towards the transducer, and the remaining weakened signal is transmitted distally until it encounters an impedance mismatch again. The position of the impedance mismatch can be determined based on the time between the ultrasound beam's emission and detection because the sound wave velocity is constant in all soft tissues [35]. Since the ratio of transmitted to reflected ultrasound energy varies depending on the properties of the tissue, different types of tissues can be differentiated.

Blood flow within the cardiovascular system can be recorded by Doppler echocardiography [35]. The Doppler effect is based on the physical phenomenon that the reflected frequency of a sound wave increases when an

object moves towards the observer and decreases when an object moves away from the observer. The difference between the transmitted and reflected frequencies is called the Doppler shift, and this shift is used to calculate the velocity of the blood flow. With pulsed wave Doppler, the piezoelectric crystals alternate rapidly between emitting and detecting short pulses of ultrasound. Since the velocity of sound in soft tissues is constant, the location of the pulse wave reflection can be determined. With pulsed wave Doppler, the velocity and direction of blood flow can be determined at a specific distance from the transducer. However, the maximum blood flow velocity that can be measured is limited because this is bounded by the pulse repetition frequency (PRF). The detector of ultrasound waves needs two samples per wavelength quarter to determine the direction and frequency of the reflected pulse wave. The highest appropriately interpretable frequency is half the PRF, also called the Nyquist frequency. With continuous wave (CW) Doppler, ultrasound waves are continuously emitted and detected by using two different sets of piezoelectric elements [35]. This allows for higher velocities to be measured; however, it is not possible to determine the location of the measured velocities. The CW Doppler yields a spectral curve that is formed by all velocities along the Doppler line.

The echocardiography parameters used for the evaluation of AS severity according to the European Society of Cardiology are: the mean pressure gradient over the aortic valve ( $PG_{mean}$ ), the aortic valve area (AVA), and the peak velocity over the aortic valve ( $v_{max}$ ). In addition, several other echocardiography parameters can be affected by the presence or progression of AS. The echocardiography parameters associated with AS progression will be described in the following paragraphs.

### Mean pressure gradient over the aortic valve

The  $PG_{mean}$  is the mean difference between the left ventricular pressure and the aortic pressure during left ventricular ejection. This parameter is determined by CW Doppler [36]. The progression of aortic valve obstruction, leads to an increased left ventricular pressure and therefore the  $PG_{mean}$  becomes higher.

### Aortic valve area

The AVA must be derived from the continuity equation, which is a fundamental principle stating that the flow into a tube is equal to the flow out of the tube [37]. In the context of the aortic valve, the stroke volume through the left ventricular outflow tract (LVOT) also passes the stenotic aortic valve opening. Consequently, to calculate the AVA, the LVOT area, the peak velocity in the LVOT, and the peak velocity over the aortic valve must be measured. To include the complete velocity during systole, instead of only the peak velocity, some experts state it is better to use the LVOT velocity-time integral (VTI) and aortic valve VTI. The VTI is the integral of the spectral curve and indicates the distance that blood has traveled during the flow period [38].

### Aortic valve peak velocity

The  $v_{max}$  is the peak velocity over the aortic valve determined by CW Doppler. Blood accelerates prior to the point of maximal obstruction. With progression of AS, the valve becomes more restricted, and consequently the  $v_{max}$  becomes higher [36].

### Left ventricular ejection fraction

The LVEF is the main parameter in assessing the left ventricular systolic function. The LVEF is the fraction of the end-diastolic volume in the left ventricle that is ejected during the systole. Left ventricular systolic dysfunction is a consequence of severe pressure overload caused by AS. To compensate for the excessive left ventricular afterload due to aortic valve obstruction, the left ventricle becomes hypertrophic to normalize wall stress [39]. However, when wall stress exceeds the compensating mechanism, the left ventricular contractile function and LVEF decline [40]. Patients with asymptomatic severe AS and an LVEF below 50% are eligible for aortic valve replacement [2].

### Left ventricular ejection time

Left ventricular ejection time (LVET) is the duration of blood flow across the aortic valve during the systole. This parameter can be affected by preload, afterload, heart rate, and contractile state of the heart [32]. LVET decreases with mitral valve regurgitation and left ventricular heart failure due to a decreased forward stroke volume. LVET increases in case of AS and high cardiac output states [41].

### Acceleration time

The acceleration time (AT) is the time interval between the initial systolic flow and its peak velocity. Severe AS is characterized by a delay and reduction in the upstroke of the aortic pressure due to the higher aortic valve pressure gradient [42]. The AT is measured with CW Doppler.

### Dimensionless index

The dimensionless index (DI) is the ratio between the LVOT VTI and the aortic valve VTI. In contrast to the measurement of the AVA, the DI does not require measurement of the LVOT cross-sectional area, which is a major cause of measurement errors [43]. In patients with AS the velocity over the aortic valve increases and therefore the DI will decrease. A DI value below 0.25 is associated with an excess risk of adverse events after diagnosis of AS and a higher risk of mortality in patients with low-gradient ( $PG_{mean} \leq 40 \text{ mmHg}$ ) severe AS and preserved LVEF [43, 44].

## First study

# Toward remote monitoring of aortic valve stenosis: wrist-derived photoplethysmography signal analysis during transcatheter aortic valve implantation

### Abstract

**Objective:** This study explores the association between aortic valve stenosis (AS) and the photoplethysmography (PPG) signal, aiming to develop a noninvasive tool to remotely monitor AS progression. PPG is a technique that is often used in wearable monitoring devices. The features of the PPG signal correlate with various physiological measurements affected by AS. Transcatheter aortic valve implantation (TAVI) offers a valuable clinical situation to unravel the effect of AS on the PPG signal characteristics. By comparing the PPG signal before and after valve implantation in patients with severe AS, the study aims to understand how valve obstruction impacts the signal.

**Methods:** This is an observational, prospective, multicenter study. Patients were included if they underwent a TAVI procedure, fitted the wristband, and were 18 years or older. Those with significant subclavian artery stenosis or a medical condition that would interfere with wearing the wristband were excluded. Participants were equipped with a wristband incorporating a PPG sensor (CE-certified Cardiowatch 287-2). The PPG data and reference data were obtained during the TAVI procedure. Participants were excluded from the analysis in case of atrial fibrillation, insufficient PPG data quality, frequent gaps in the PPG data, or unsaved PPG data. The PPG data were filtered and high-amplitude motion artifacts were removed. Subsequently, 300 consecutive cardiac cycles were detected with an automated algorithm. Twenty-two features were extracted from the selected cardiac cycles before and after valve placement. The features were compared before and after valve placement by their medians and interquartile ranges and by performing a Wilcoxon-Signed Rank test.

**Results:** In total, 237 patients were included in the study. After exclusion due to atrial fibrillation (n=27), poor quality of the PPG data (n=36), frequent data gaps caused by disconnection (n=6) or missing PPG data (n=12), 156 patients remained for the analysis. The study population had a mean age of  $80 \pm 6.3$  years, and 56% were female. A significant increase after valve placement was found for the PPG features: systolic amplitude, area under the curve, upstroke, downstroke, heart rate, (b+e)/a ratio, and the b/a ratio. A significant decrease after valve placement was found for the PPG features: crest time, e/a ratio, notch time, and the pulse width of the PPG signal at different heights.

**Conclusion:** After valve implantation in patients with severe AS, significant differences in the PPG signal characteristics were identified. These findings suggest that the PPG signal characteristics could be used as potential indicators of AS progression, including a reduced systolic amplitude or an increased crest time. Although these results are promising, future research should demonstrate whether similar differences are found under nonsurgical conditions, in native aortic valve disease, and with gradual AS progression. If so, the wrist-derived PPG signal will offer potential for remote monitoring of patients with AS.

## 4.1 Introduction

Aortic valve stenosis (AS) has a poor prognosis once patients become symptomatic, often when the disease is in a severe stage, with two-year and five-year survival rates of 50% and 25%, respectively [45]. Even without symptoms, severe AS carries worse outcomes, and valve replacement may be indicated [2]. Patients undergo repeated echocardiographic examinations to monitor AS progression since there is no effective medical therapy to halt disease progression. According to the European Society of Cardiology (ESC) guidelines, asymptomatic patients with severe AS should be followed up every six months, patients with moderate AS at least annually, and patients with mild AS every two to three years [2]. This disease monitoring process imposes high costs and burdens on healthcare professionals and patients. A noninvasive tool to detect severe AS or remotely monitor AS progression could improve disease management and make the follow-up trajectory more efficient.

Photoplethysmography (PPG) sensors are frequently used in wearable devices to monitor vital parameters, such as heart rate and oxygen saturation [5]. The hypothesis is that the PPG waveform could be used to remotely monitor AS progression, as its features correlate with various physiological measurements affected by AS. For instance, the progression of AS can result in a reduced stroke volume, delayed pulse upstroke, and autonomic dysfunction [11], all of which can be assessed through the characteristics of the PPG signal [7, 10, 46].

Given the above, it seems prudent to study the relationship between the PPG signal and AS to develop a remote monitoring tool for AS. It is hypothesized that transcatheter aortic valve implantation (TAVI) offers a valuable clinical situation to unravel the effect of PPG on the presence of AS. By comparing PPG signals pre- and post-valve implantation, it can be determined if wrist-derived PPG signal characteristics provide information on the function of the aortic valve. This study investigates the acute changes in the PPG signal characteristics induced by TAVI to understand how valve obstruction impacts the

signal. This exploratory study takes the initial steps towards a remote monitoring tool for AS.

## 4.2 Method

This is an observational, retrospective, multicenter study. Data were collected from patients hospitalized for a TAVI procedure in the Radboudumc or the Erasmus Medical Center from March 2022 to April 2023. Inclusion criteria were: undergoing a TAVI procedure, fitting the wristband, and being 18 years or older. Individuals were excluded if they had significant subclavian artery stenosis or any medical condition that would interfere with wearing the wristband.

An overview of the performed method can be found in the flowchart in Figure 9. Preprocessing and feature extraction of the data were performed using Python 3.8 *PPG-sensor*(Python Software Foundation, Wilmington, United States) . The statistical analysis was performed using SPSS Statistics 27 (IBM, Armonk, USA).

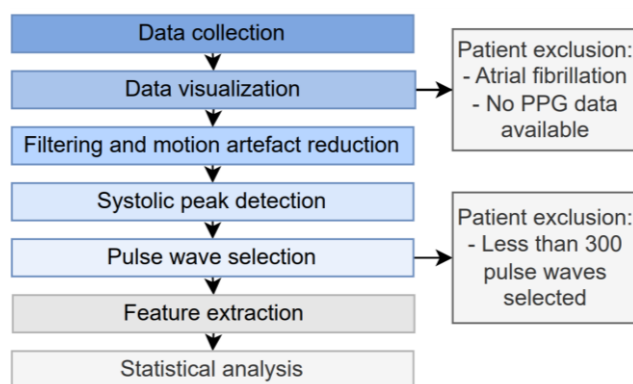


Figure 9: Overview of the performed method. Patients could be excluded during two steps in the data analysis; after data visualization and after the pulse wave selection according to the exclusion criteria described in the grey blocks.

### 4.2.1 Data collection

The green, red, and infrared PPG signals were obtained at the wrist with the Cardiowatch 287-2 (Corsano Health, Den Haag, The Netherlands) with a sampling frequency of 128 Hz. In Figure 10, the design of the Cardiowatch can be seen [47]. The wristband was attached in the cardiac catheterization room prior to the TAVI procedure and detached afterwards. PPG data was collected during the entire procedure.

Reference data were acquired by simultaneous electrocardiogram (ECG) recordings and invasive blood pressure measurements routinely obtained during the procedure with a sampling frequency of 2000 Hz (Sensis, Siemens Healthineers) or 250 Hz (ICM+, University of Cambridge).



Figure 10: The Cardiowatch 287-2 with the PPG sensor on the back of the wristband in the picture on the right.

Echocardiographic data were collected around one month before and after the TAVI procedure. Collected demographic data included gender, age, Body Mass Index (BMI), hair density on the lower arm/wrist, wrist circumference, and presence of peripheral artery disease or other cardiac diseases.

### 4.2.2 Data visualization and exclusion

The green, red, and infrared PPG data and the reference data were visualized. After visualization of the PPG signal, the decision was made to use the green and infrared PPG signals for further analysis. The red PPG signal was excluded because the signal quality was poor for this LED color. Green light has a lower penetration depth than red and infrared light, and is therefore less prone to artifacts and the systolic peaks are prominent and easy to detect. However, this green light is less sensitive to small changes in blood volume, making it difficult to identify the dicrotic notch of this signal [22, 24]. Therefore, the infrared PPG signal was chosen to extract morphology characteristics of the signal, and the green PPG signal was chosen to extract the frequency characteristics.

Patients showing atrial fibrillation on their ECG were excluded from the study, as this affects the morphology of the PPG pulse waves [48]. Patients were excluded from further analysis when PPG data were missing or in case of insufficient PPG quality. Quality was defined as insufficient if it was impossible to extract 300 good-quality cardiac cycles from the PPG signal using the method

described in Section 4.2.3. This approach is similar to the methods used in various studies in the literature that focus on assessing the quality of the PPG signal [49, 50]. Assuming that at least 1200 pulse waves were recorded before and after valve placement (corresponding to 20 minutes at a heart rate of 60 beats per minute), the signal was annotated as low quality if more than 75% of the PPG data was corrupted.

### 4.2.3 PPG signal preprocessing

#### Filtering and removing motion artifacts

The PPG signal was filtered by a bandpass filter with cutoff frequencies of 0.5 Hz and 5 Hz to eliminate respiratory rate and noise and preserve the heart rate range (30 - 300 beats per minute).

Movement can disrupt skin-sensor contact, leading to the incidence of ambient light on the PPG sensor. This results in movement artifacts which can be seen as high amplitude variations in the PPG signal. To reduce the impact of these motion artifacts on the performance of the peak detection algorithm, the PPG signal was set to zero whenever movement was detected. The movement artifacts were detected with the use of the Hilbert transform. The Hilbert transform can extract the envelope from a modulated signal. In other words, it finds all maxima and minima and draws a line between these points. The absolute value of this envelope can be seen as a representation of the signal amplitude. Whenever the height of the envelope exceeded a predefined threshold, the signal was set to zero. The movement threshold, set at four times the envelope's mean amplitude, was determined through experimentation. This particular threshold achieves an optimal balance between being sensitive enough to identify motion artifacts and remaining conservative in its approach to avoid mistakenly discarding valid PPG data.

#### Peak detection algorithm

Systolic peak detection was based on the “Event-related Moving Averages with Dynamic Threshold” method described by Elgendi et al. [51]. This method consists of three steps: squaring, identifying the regions of interest, and classifying

the systolic peaks using thresholds. A schematic overview of this method can be found in Figure 11.

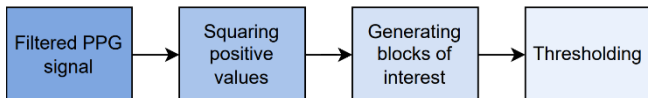


Figure 11: The stepwise method for systolic peak detection.

### Squaring

This step involved setting all negative values to zero and squaring the remaining signal. In this way, large variations resulting from systolic waves were emphasized and the more minor differences due to diastolic peaks or noise were suppressed.

### Generating blocks of interest

Two moving average thresholds were used to determine the region of interest where the systolic peak should be located. The first moving average ( $MA_{peak}$ ) was used to identify the systolic peak area and is given by Equation 1:

$$(1) \ MA_{peak}[n] = \frac{1}{W_1} (y[n - \frac{W_1-1}{2}] + \dots + y[n] + \dots + y[n + \frac{W_1-1}{2}]),$$

with  $W_1$  the window size of the minimum systolic peak duration and  $y[n]$  the squared signal at sample number  $n$ . The value of  $W_1$  is defined as 111 milliseconds, which was determined after a brute-force search by Elgendi et al.  $MA_{peak}$  is plotted as the blue line in Figure 12.

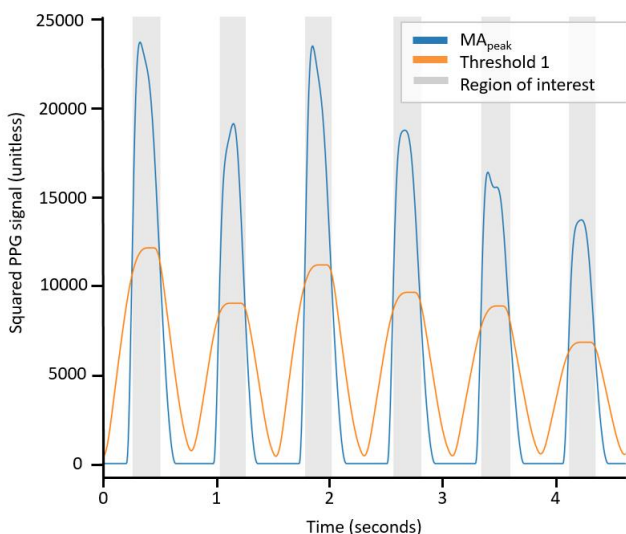


Figure 12: The blue line represents the  $MA_{peak}$  which is calculated based on the squared PPG signal and negative values set to zero. The orange line represents the first dynamic threshold calculated by Equation 3. The grey blocks are the regions of interest located where  $MA_{peak}$  exceeds the first dynamic threshold.

The second moving average ( $MA_{beat}$ ) was used to emphasize the heartbeat area and is given by Equation 2:

$$(2) \ MA_{beat}[n] = \frac{1}{W_2} (y[n - \frac{W_2-1}{2}] + \dots + y[n] + \dots + y[n + \frac{W_2-1}{2}]),$$

with  $W_2$  the moving average window, and  $y[n]$  the squared PPG signal at sample number  $n$ . The value for  $W_2$  was equal to 667 milliseconds, representing approximately one heartbeat duration if the heart rate is 90 beats per minute. This window size was also determined after a brute-force search by Elgendi et al. [19]

The first dynamic threshold was calculated using Equation 3:

$$(3) \ Threshold_1 = MA_{beat}[n] + \alpha,$$

with  $MA_{beat}[n]$  the moving average at sample  $n$ , and  $\alpha$  the offset level calculated by  $\beta * \bar{z}$ .  $\beta$  equals 0.02, and  $\bar{z}$  was the statistical mean of the squared PPG signal.

The first dynamic threshold is plotted as the orange line in Figure 12. The regions of interest are located where  $MA_{peak}$  exceeds the first dynamic threshold, as can be seen in Figure 12 by the gray squares.

### Thresholding

A second threshold was used to reduce the number of regions holding noise or diastolic peaks instead of systolic peaks. This second threshold is equal to the value of  $W_1$ , which corresponds to the minimum systolic wave duration of 111 ms.

$$(4) \ Threshold_2 = W_1$$

Regions with a duration below this threshold were classified as noise and subsequently discarded. In the remaining regions, the systolic peaks were identified as the maximum value within each region.

In addition, the peaks were rejected if their peak-to-peak interval was below the third threshold, as described by:

$$(5) \ Threshold_3 = \frac{t_{pp\ mean}}{2},$$

with  $t_{pp\ mean}$  being the mean peak-to-peak interval of the entire PPG signal. This threshold is based on

the assumption that a degree of regularity should exist in the time interval between consecutive peaks. Applying this criterion excluded periods of rapid pacing (180-220 beats per minute) during the TAVI procedure.

#### Segment selection algorithm

After the systolic peak detection, the signal was separated into segments of individual pulse waves, from the valley before the systolic peak to the valley after the systolic peak. Figure 13 illustrates an individual pulse wave of the PPG signal. The valleys before and after the systolic peak were identified by inverting the signal and running the signal through the peak detection algorithm.

Nine rejection criteria were used to identify segments with low-quality PPG signals using the methods of Fischer et al. [49] and Liu et al. [50]. If the pulse wave segment complied with one of the criteria, the segment was removed. The criteria were based on four characteristics of the PPG pulse, as shown in Figure 12, including the systolic amplitude (SA), the pulse wave duration (PWD), the crest time (CT) and the systolic-to-diastolic duration ratio (SDR). The CT, also known as the systolic duration, is used to calculate the SDR.

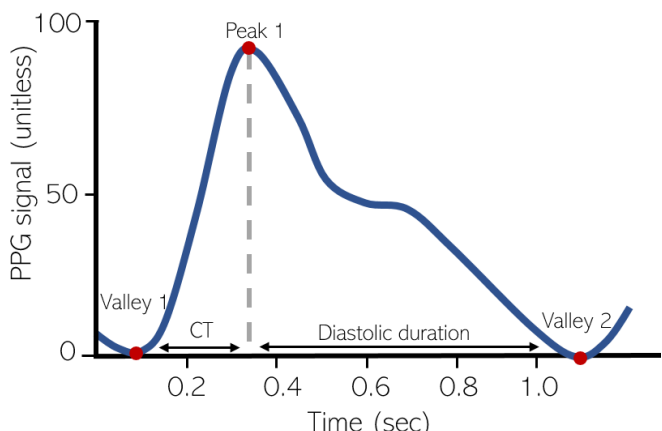


Figure 13: The characteristics of the PPG pulse wave. This figure is modified from [50]. CT = crest time.

These characteristics are defined as follows (A = amplitude, T = time):

- (1)  $SA_{left} = A_{peak1} - A_{valley1}$
- (2)  $SA_{right} = A_{valley1} - A_{valley2}$
- (3)  $PWD = T_{valley2} - T_{valley1}$
- (4)  $CT = T_{peak1} - T_{valley1}$

The segments are rejected if they comply with one of the following criteria based on literature-reported values:

1. CT is less than 0.08 seconds or more than 0.49 seconds [52].
2. SDR is above 1.1 [53, 54].
3. The minimum of  $\frac{PWA_{right}}{PWA_{left}}$  or  $\frac{PWA_{left}}{PWA_{right}}$  is below 0.4 [50].
4. PWD is greater than 2 seconds or less than 0.3 seconds (pulse rate from 30 to 200 beats per minute) [50].
5. The number of minima and maxima in the segment is above five [49].

In addition to these conditions, we also considered three rejection criteria based on the features of the neighbor pulses. Cardiac cycles that do not show a high similarity with their consecutive pulse are rejected based on the following three conditions, with  $n$  representing the  $n$ th pulse:

1. The ratio of  $CT(n-1)$  and  $CT(n)$  is out of the range of 33% to 300% [49].
2. The ratio of  $PWD(n-1)$  and  $PWD(n)$  is out of the range of 33% to 300% [55].
3. The ratio of  $PWA(n-1)$  and  $PWA(n)$  is out of the range of 50% to 200% [49].

Three hundred consecutive heartbeat segments were selected from the remaining segments before and after valve implantation to calculate the features.

#### 4.2.4 Feature extraction of PPG signal

Table 2 shows an overview of the extracted features. Time-domain features were extracted per pulse wave, leading to 300 feature values before and after valve implantation. Frequency features were extracted from 300 consecutive pulse waves, leading to one value before and after valve implantation. Since the systolic peaks are more prominent in the PPG signal obtained by green light, this signal was used to extract the frequency features and the crest time. The morphology features were extracted from the PPG signal obtained by infrared light. Heart rate-dependent features were corrected by dividing the feature value by the peak-to-peak interval ( $t_{pp}$ ) of the

corresponding peak and its neighboring peak. Corrected heart rate-dependent features were: AUC, upstroke, downstroke, pulse width, and crest time. The systolic amplitude depends on the LED strength of the sensor. Therefore, this feature is corrected by dividing it by the LED strength.

Since the PPG signal amplitude depends on internal factors (e.g. blood volume, vascular tone) and external factors (e.g. skin-sensor contact, LED strength), the baseline amplitude varies widely between patients. Therefore, the amplitude-related features (systolic amplitude, IPA, AUC, upstroke, and downstroke) are standardized. The values are standardized by Equation 10, in which the mean and standard deviation were calculated based on the 300 feature values before valve implantation. This state is taken as the baseline since the effect of the novel biological valve is investigated compared to the normal situation for the patient suffering from severe AS.

$$(5) \text{ standardized value} = \frac{\text{value} - \text{mean}_{\text{before}}}{\text{STD}_{\text{before}}}$$

In patients with atherosclerosis and vascular aging the dicrotic notch becomes less prominent and the diastolic peak disappears [56]. The calculations of the features stiffness index, IPA, augmentation

index, and notch time depend on the position of one of these morphological landmarks. Therefore, these features were calculated only for pulse waves showing a dicrotic notch or diastolic peak. Consequently, these features were not calculated for all 300 heartbeats in most patients. Nevertheless, each patient showed multiple pulse waves containing the diastolic peak or dicrotic notch, enabling computation of these features for analysis.

#### 4.2.5 Statistical analysis

For both groups (before and after implantation), the features were visually tested for normality with histograms and Q-Q plots. In case of a normal distribution, the mean and standard deviation (SD) were calculated. In case of a nonnormal distribution, the median and interquartile range (IQR) were calculated. Subsequently, it was assessed if there were significant differences between before and after valve implantation using a paired T-test or a Wilcoxon signed-rank test, whichever was appropriate. Differences were considered significant in the case of a p-value below 0.05. The results were visualized using bar charts and PPG plots before and after valve implantation.

Table 2: Description of the 22 extracted PPG signal features, including their domain and the PPG LED channel used for extraction. A more detailed description of the features can be found in Chapter 3.

Feature	Domain	PPG channel	Description
Systolic amplitude	Time	Infrared	Amplitude of the systolic peak
AUC	Time	Infrared	Area under the curve
Augmentation index	Time	Infrared	Ratio of the diastolic and systolic amplitude
Stiffness index	Time	Infrared	A patient's height divided by the time between the systolic and diastolic peak
IPA	Time	Infrared	Ratio between the systolic and diastolic area
Upstroke	Time	Infrared	Slope from the start of the pulse wave towards the systolic peak
Downstroke	Time	Infrared	Slope from the systolic peak towards the end of the pulse wave
Pulse width 50%	Time	Infrared	Pulse width at 50% of the height of the systolic peak
Pulse width 60%	Time	Infrared	Pulse width at 60% of the height of the systolic peak
Pulse width 70%	Time	Infrared	Pulse width at 70% of the height of the systolic peak
Pulse width 80%	Time	Infrared	Pulse width at 80% of the height of the systolic peak
Pulse width 90%	Time	Infrared	Pulse width at 90% of the height of the systolic peak
Notch time	Time	Infrared	Time interval from the foot of the waveform to the dicrotic notch
B/A ratio	Time	Infrared	Ratio between the <i>b</i> and <i>a</i> amplitudes of the second derivative of the pulse wave
E/A ratio	Time	Infrared	Ratio between the <i>e</i> and <i>a</i> amplitudes of the second derivative of the pulse wave
BE/A ratio	Time	Infrared	Ratio between the <i>b</i> * <i>e</i> and <i>a</i> amplitudes of the second derivative of the pulse wave
Crest time	Time	Green	Time interval from the foot of the waveform to the systolic peak
Peak-to-peak interval ( $t_{pp}$ )	Time	Green	Distance between two consecutive systolic peaks
SD of $t_{pp}$	Time	Green	Standard deviation of the peak-to-peak intervals
Beats per minute	Frequency	Green	Heart rate
Low-frequency %	Frequency	Green	Percentage of the low-frequency (0.05 - 0.15 Hz) power compared to the total power spectrum (0-0.5 Hz)
High-frequency %	Frequency	Green	Percentage of the high-frequency (0.15 - 0.5 Hz) power compared to the total power spectrum (0-0.5 Hz)

### 4.3 Results

In total, 237 participants were included in the study. Of these participants, 27 were excluded due to atrial fibrillation, 36 were excluded due to poor quality of PPG data, six were excluded due to frequent data gaps caused by disconnection between the sensor and the server, and twelve were excluded due to missing PPG data. Figure 14 shows an example of a good quality PPG signal (top) and an example with poor quality PPG signal (bottom). The descriptive statistics of the patients who were excluded due to insufficient PPG data quality can be found in Appendix B.1.

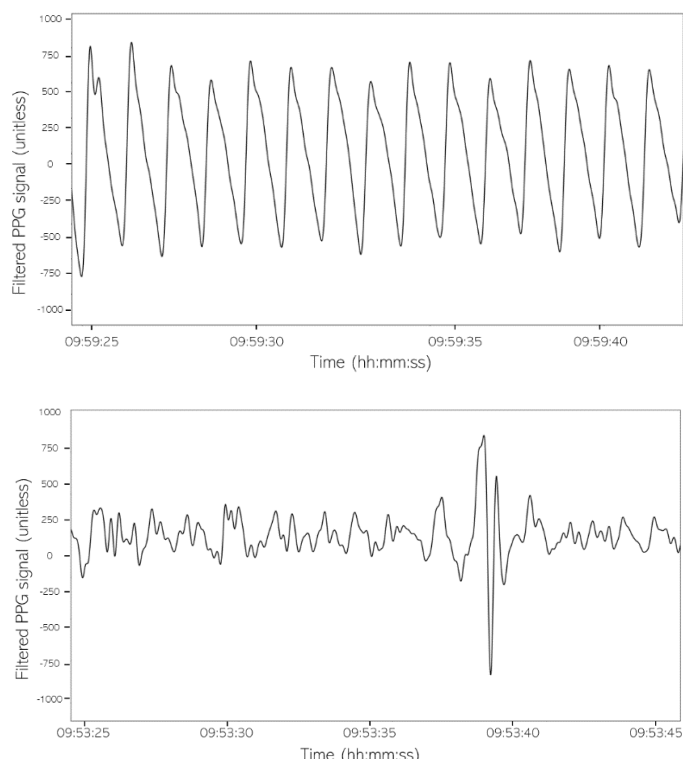


Figure 14: Examples of a good-quality PPG signal (on top) and a low-quality PPG signal (bottom)

The remaining study population consisted of 156 patients who underwent TAVI with a mean age of  $80 \pm 6.3$  years, and 56.4% were female. Patients suffered from different comorbidities, such as hypertension (52.6%), diabetes (28.2%), moderate or severe aortic regurgitation (18.8%), and coronary artery disease defined by a previous coronary artery bypass grafting (CABG), percutaneous coronary intervention (PCI), stenosis of more than

70% or a previous myocardial infarct (44.2%). The baseline characteristics of this population can be found in Table 3.

Table 3: Descriptive statistics of the study population. Values are n(%), means  $\pm$  standard deviation or medians (interquartile range) AR = aortic valve regurgitation. \*Defined by a previous myocardial infarction, CABG or PCI, or stenosis  $> 70\%$

Characteristic	Statistic	N
Age (years)	80 ( $\pm 6.3$ )	156
Female gender	88 (56.4)	156
BMI ( $\text{kg}/\text{m}^2$ )	26.9 (24.0 - 29.4)	156
LVEF prior to TAVI (%)	52 $\pm 11.9$	87
Coronary artery disease*	69 (44.2)	156
Moderate or severe AR	20 (18.8)	156
Peripheral artery disease	15 (9.6)	156
Hypertension	82 (52.6)	156
Diabetes	44 (28.2)	156
Former or current smoker	88 (59.5)	148

The calculated PPG characteristics did not follow a normal distribution. The median and IQR of the green and infrared PPG signal characteristics can be found in Table 4. A significant difference before and after valve implantation was demonstrated for the PPG variables: heartbeats per minute (BPM), crest time, systolic amplitude, AUC, b/a ratio, b/e ratio, be/a ratio, upstroke, downstroke, pulse width at all heights (50-90%), and the time the dicrotic notch occurred during the cardiac cycle.

The IQRs before and after valve implantation show overlap for every feature. The crest time exhibits minimal overlap, with the median after valve implantation positioned at the 25<sup>th</sup> percentile of the crest time before valve implantation.

## First study

Table 4: Median and interquartile range (IQR) of the features extracted from the infrared and green PPG signal before and after valve implantation. The p-value was retrieved with a Wilcoxon-Singed Rank test. IPA = inflection point ratio, PW = pulse width,  $t_{pp}$  = peak-to-peak interval.

	Before		After		
	Median	IQR	Median	IQR	p-value
<i>PPG features derived from the infrared PPG signal</i>					
Systolic amplitude	62.334	41.251 - 95.132	81.910	50.315 - 124.471	<0.001
AUC/ $t_{pp}$	62.353	42.782 - 94.679	77.782	49.100 - 121.239	<0.001
B/A ratio	-2.331	-4.233 - -1.560	-1.816	-2.636 - -1.158	<0.001
E/A ratio	1.747	0.970 - 3.109	1.113	0.686 - 2.061	<0.001
BE/A ratio	-4.207	-8.184 - -2.600	-3.095	-4.860 - -1.975	<0.001
Augmentation index	0.677	0.612 - 0.761	0.660	0.583 - 0.750	0.356
Stiffness index	600.838	477.918 - 737.084	601.232	494.094 - 719.926	0.931
IPA	3.373	1.211 - 6.601	3.564	1.412 - 7.556	0.233
Upstroke / $t_{pp}$	465.759	301.352 - 646.602	652.964	438.056 - 1085.725	<0.001
Downstroke / $t_{pp}$	222.878	152.342 - 304.047	278.089	187.374 - 479.233	<0.001
PW 50% / $t_{pp}$	0.473	0.429 - 0.510	0.448	0.403 - 0.500	0.003
PW 60% / $t_{pp}$	0.401	0.357 - 0.433	0.366	0.320 - 0.421	<0.001
PW 70% / $t_{pp}$	0.320	0.280 - 0.350	0.288	0.254 - 0.332	<0.001
PW 80% / $t_{pp}$	0.235	0.205 - 0.263	0.214	0.189 - 0.242	<0.001
PW 90% / $t_{pp}$	0.151	0.132 - 0.165	0.137	0.122 - 0.156	<0.001
Notch time	0.455	0.421 - 0.487	0.442	0.397 - 0.475	<0.001
<i>PPG features derived from the green PPG signal</i>					
Beats per minute	66.142	58.117 - 75.971	67.334	60.513 - 76.733	0.015
SD of $t_{pp}$ interval	47.002	33.571 - 72.612	45.562	31.008 - 72.982	0.670
Low-frequency %	15.558	9.962 - 23.640	17.566	10.425 - 27.149	0.078
High-frequency %	53.641	33.397 - 69.056	55.604	32.337 - 71.373	0.700
Crest time / $t_{pp}$	0.333	0.307 - 0.364	0.307	0.281 - 0.331	<0.001

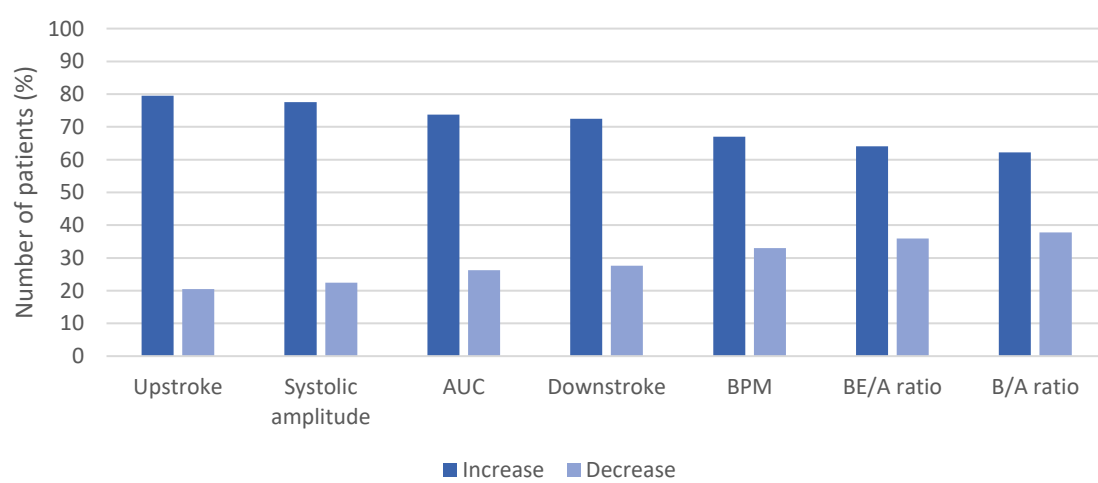


Figure 15: Bar chart of the PPG signal features that show a significant increase after valve placement. AUC = area under the curve, BPM = beats per minute.

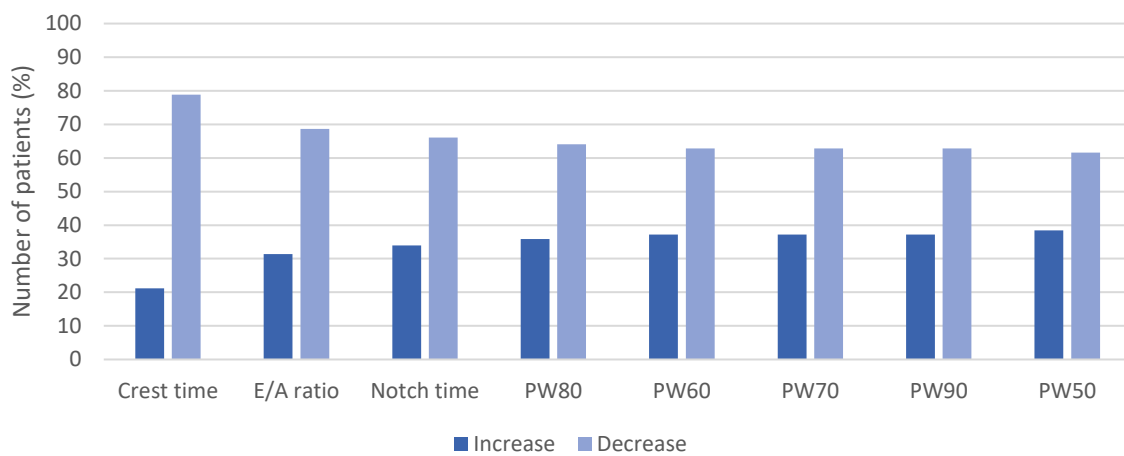


Figure 16: Bar chart of the PPG signal features that show a significant decrease after valve placement. PW = pulse width at a percentage of the systolic peak height.

Figure 15 shows the percentage of patients demonstrating a significant increase in the PPG signal characteristics after valve implantation. The percentage of patients who demonstrated a significant decrease in the PPG signal characteristics after valve implantation can be found in Figure 16. An increase was found in more than 70% of the patients after valve implantation for the following PPG features upstroke, systolic amplitude, AUC, and downstroke. A decrease was found in almost

80% of the patients after valve implantation for the crest time.

Figure 17 shows four examples of the PPG signal for a patient with severe AS before (dashed line) and after (continuous line) TAVI. In these curves, it can be seen that the crest time, the notch time, and the pulse width decrease, while the systolic amplitude, AUC, upstroke, and downstroke increase.

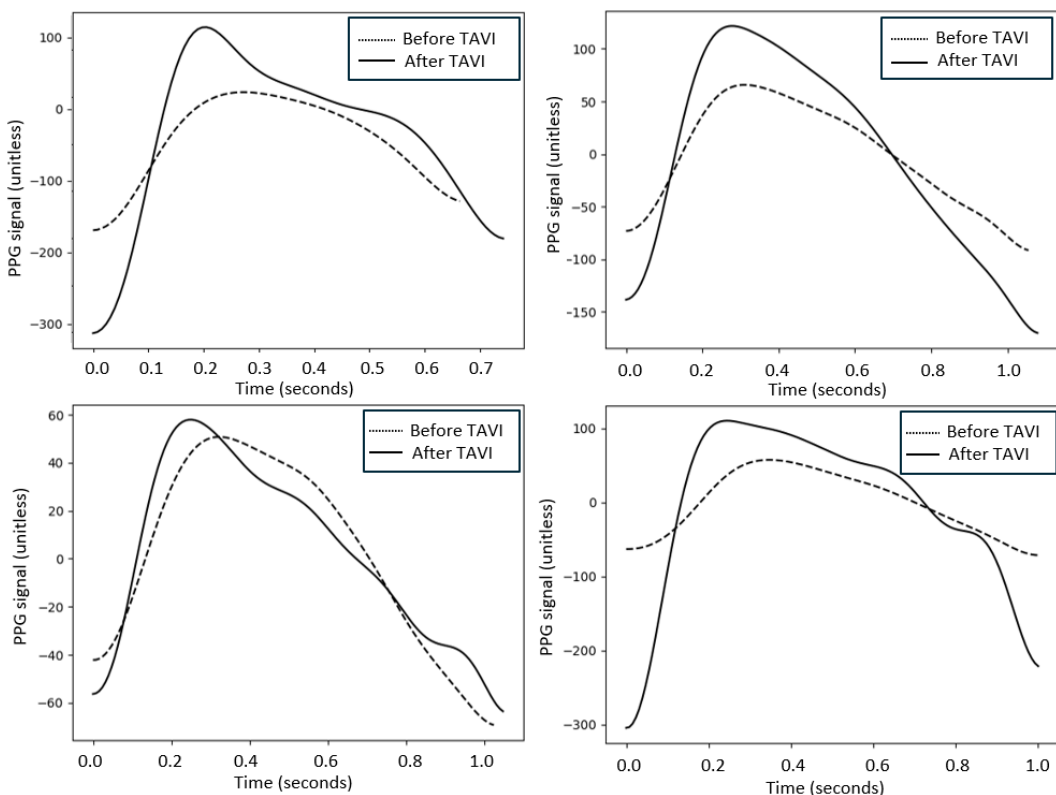


Figure 17: Examples of the PPG signal before (dashed line) and after (continuous line) TAVI. After TAVI, the crest time and pulse width decrease, and the systolic amplitude, AUC, upstroke and downstroke increase. The x-axis represents the pulse wave duration, not real-time. The PPG segments are plotted from the onset of the pulse waves (starting at time = 0 seconds) to the end of the pulse wave.

## 4.4 Discussion

### 4.4.1 Summary of findings

To study the PPG signal, we developed an algorithm to select 300 high-quality PPG pulse waves and extract features. PPG signal characteristics have been compared before and after valve implantation to assess the effect of valve placement in patients with severe AS on the PPG signal. PPG signal characteristics markedly differ prior to and after valve implantation in patients with severe AS. After reversal of the severe aortic valve obstruction by implantation of a biological aortic valve, the PPG signal had a higher systolic amplitude, faster upstroke and downstroke, and a larger AUC in more than 70% of the patients. A significantly reduced crest time was found in almost 80% of the patients. These findings are in line with the observed differences in the aortic pressure curve after valve implantation in patients with severe AS, and warrant further investigation as to whether wrist-derived PPG can be used to remotely monitor AS progression [19].

Wrist-derived PPG has demonstrated its value in the at-home monitoring of patients with cardiovascular disease. These noninvasive wearables have been used for the detection of atrial fibrillation, continuous monitoring of heart rate and oxygen saturation, and to calculate the heart rate variability [5, 32, 57].

In previous studies, the PPG signal has been demonstrated to correlate with stroke volume, autonomic function, the LVET, and blood pressure [25, 33, 51, 58]. Given the impact of AS on the hemodynamics, we hypothesized that the morphology of the PPG signal is affected in severe AS. TAVI offers a unique setting to study the relation between AS and the PPG signal within a patients. Our results clearly demonstrate that the PPG signal characteristics change after valve implantation in patients with severe AS, which highlights the potential of PPG in monitoring AS.

### 4.4.2 Interpretation of results

The significant increase in systolic amplitude could be attributed to an increased blood volume reaching the PPG sensor, which could, in turn, be caused by increased cardiac output. Previous

research on the acute hemodynamic effects of a TAVI procedure has demonstrated an increased cardiac output after valve implantation, supporting this interpretation [19]. Furthermore, the heart rate increases significantly after valve placement increasing the cardiac output. The AUC, upstroke, and downstroke depend on the systolic amplitude; therefore, these features also increase. The cardiac output decreases gradually with the progression of AS due to chronic pressure overload of the left ventricle [40]. Thus, a decrease in these variables could be a potential marker of decreased cardiac output, which could indicate AS progression. However, a decreased cardiac output is of course affected by a lot of conditions different than AS and therefore the clinical value would be to monitor progression and not detect AS.

The crest time decreases after valve implantation, meaning that the maximum blood volume at the measuring site is reached earlier in systole. The crest time depends on blood pressure, vascular tone, and cardiac output. The crest time is elongated in patients with hypertension compared to healthy individuals [22]. Since valve implantation is associated with an immediate increase in aortic systolic blood pressure, crest time is also expected to increase [19]. Surprisingly, a significant decrease is observed. This suggests a factor exerting a more substantial impact on the crest time than elevation of the blood pressure. Possible factors contributing to the decreased crest time are shorter ejection time, vasodilation, or increased cardiac output. The progression of AS can reduce cardiac output and prolong ejection time. This suggests that an increased crest time could function as an indicator of AS progression. However, the effect of vasodilation or vasoconstriction on the crest time must be eliminated.

Awad et al. [26] have shown that an increase in systemic vascular resistance (SVR), resulted in an increased width of the PPG pulse wave, consistent with a prolongation of the time it takes for the PPG pulse wave to reach the arteriolar vessels. This study shows that the pulse width decreases significantly after valve placement. This contradicts the findings of Yotti et al. [21], who observed an increase in SVR after TAVI procedures in patients

with severe AS. This suggests that the pulse width is decreased due to a factor with greater impact than the increased SVR. A possible explanation could be that the time required to reach the arterioles is reduced, due to the shortened ejection time after resolving the aortic valve obstruction. Consequently, increased pulse width could serve as a potential indicator of AS progression. However, it is important to consider the effect of SVR on the pulse width before drawing conclusions regarding AS progression.

The notch time decreases after valve implantation. The dicrotic notch is the result of the reflection wave occurring due to impedance differences between the elastic arteries and the inelastic capillaries. An earlier occurring notch time would indicate a faster reflection wave, which could be due to stiffer arteries [22]. Since it is unlikely that the vascular stiffness properties change acutely after valve implantation, this does not explain the significantly decreased notch time. The location of the dicrotic notch vaguely corresponds to the closure of the aortic valve [28]. The reduced notch time may be explained by the earlier aortic valve closure due to the faster achieving aortic peak pressure after TAVI [19]. This suggests that an increased notch time could be used as an indicator of AS progression. However, it is important to consider that vascular stiffness increases with age, leading to a decrease in notch time. Therefore, the notch time might remain constant with vascular aging and the progression of AS. To fully understand the evolution of the notch time throughout the progression of the disease, it is recommended to conduct a longitudinal study involving the analysis of PPG signals over multiple years in individuals diagnosed with AS.

The ratios  $b/a$  and  $(b-e)/a$  increase significantly after valve placement. These ratios increase with age and reflect vascular stiffness. The  $e/a$  ratio decreases after valve implantation and has been demonstrated by Takazawa et al. [34] to decrease with increased arterial stiffness. This suggests that vascular stiffness increased after valve implantation. As mentioned before, vascular stiffness properties are unlikely to change acutely after valve implantation. This statement is also

supported by the fact that no significant differences were found for the augmentation index, stiffness index, and IPA, which are all features correlated with vascular stiffness [25].

Simonyan et al. [10] demonstrated that patients with AS have higher LF% and HF% values than healthy people of comparable age. In this study, no significant differences in LF% and HF% were found after valve implantation. This could be due to the short measuring time of 300 cardiac cycles, and therefore these frequency features should be treated with caution. Furthermore, the heart rate variability is unlikely to change acutely after TAVI and therefore it is not surprising that no significant differences were found.

### 4.4.3 Limitations

First of all, this study measured the PPG signal under surgical conditions. Administration of anesthetics during the TAVI procedure causes changes in blood pressure, vascular tone, and heart rate [59]. These factors can also affect the PPG signal. Furthermore, in many patients, rapid ventricular pacing (RVP) is induced during, pre- or post-valve implantation to decrease or diminish the cardiac output. RVP could trigger compensatory mechanisms in the cardiovascular system, potentially affecting the PPG signal. Consequently, some significant differences observed in the PPG features pre- and post-valve implantation could be attributed to the compensatory mechanisms or administration of anesthetics rather than the specific presence or absence of AS. To further investigate the association between PPG and AS, surgical conditions must be eliminated.

In addition, the findings of this study should be interpreted with caution in terms of generalizability. The study focused on patients who underwent TAVI, and the significant differences represent the acute effects of the procedure. Since there was no time for the human body to adapt to the changes, the results may be different regarding the long-term progression of AS. Moreover, during TAVI the two most extreme scenarios (severe AS vs. new biological valve) have been compared. Therefore, it is recommended to investigate whether slower progression of AS could be monitored under

---

nonsurgical conditions. This could be done with a longitudinal study that follows patients with mild AS for an extended period, potentially spanning several years.

Lastly, a high percentage (15%) of the patients were excluded due to the insufficient quality of the PPG data. It was attempted to identify the underlying cause by comparing patient characteristics such as wrist circumference, BMI, peripheral artery disease, skin type, and hair density between the patients with low- and high-quality PPG data. No clear differences in patient characteristics were found between patients with low- and high-quality, see Appendix B.1. Therefore, it remains difficult to identify the underlying cause of this high number of patients with insufficient data quality. An explanation could be incorrect skin-sensor connection due to displacement of the sensor after applying the wristband. This cannot be ascertained as the researchers were not present during the entire measurement. It is recommended to communicate this finding with the wristband developer to address potential software or hardware problems causing the low-quality PPG data.

#### 4.4.4 Future perspectives

In future studies, it is recommended to eliminate the surgical conditions introduced in this study. This could be achieved by comparing the PPG signal one day before surgery upon hospital admission with the PPG signal one day after surgery in the cardiac care unit. However, in this way, PPG data from a patient with a native stenotic valve will be compared with a novel biological valve. With the use of this technique in remote monitoring of AS, the focus should be on solely native valves and more subtle changes in AS progression. Therefore, it is suggested to perform a study in patients who undergo a clinically-indicated TTE and compare the PPG signals between patients with and without AS. This provides the situation to compare the PPG signal from patients with different stages of AS. If this study also supports the potential of PPG in AS monitoring, it should be considered to perform a

longitudinal study. By measuring the PPG signal of AS patients for multiple years, it can be validated if this sensor can be used for long-term monitoring of AS patients.

### 4.5 Conclusion

In conclusion, the findings of this study provide valuable information on the impact of valve implantation on PPG signal characteristics in patients with severe AS. This study demonstrates that PPG features, including systolic amplitude, AUC, upstroke, downstroke, pulse width, and crest time, undergo significant changes after valve implantation in patients with severe AS. These changes suggest that the characteristics of the PPG signal could be used as potential indicators of AS progression, such as a decrease in systolic amplitude or an increase in the crest time. However, the PPG features are also influenced by other conditions besides AS and therefore further research into the effect of AS on these features is required. Although the results are promising, there is a need for further research under nonsurgical conditions and with long-term monitoring to establish the association between PPG characteristics and AS.

## Second study

Toward remote monitoring of aortic valve stenosis with wrist-derived photoplethysmography: rationale and design of the DETECT-REMOTE study

---

### Abstract

**Objective:** In the previous study, we demonstrated important differences in PPG signal characteristics between severe aortic valve stenosis (AS) and a well-functioning biological aortic valve within a patient in a surgical setting of transcatheter aortic valve implantation (TAVI). To further assess the potential impact of AS on wrist-derived PPG, in the present study, we will investigate the PPG signal characteristics in relation to the presence or absence, and severity of AS in patients undergoing a clinically indicated transthoracic echocardiogram (TTE). The DETECT-REMOTE study focuses on collecting data during TTE to avoid bias introduced by surgical conditions and explore subtle differences in aortic valve function between patients.

**Methods:** The DETECT-REMOTE study is an observational, prospective, single-center study to investigate the effects of AS on the PPG signal characteristics in patients undergoing a clinically indicated TTE. Participants will be included if their age is above 18 years and if they undergo a TTE due to suspected or known AS, a bicuspid and stenotic aortic valve, or a non-stenotic native valve. Participants will be excluded if they have a significant subclavian artery stenosis. PPG data will be collected with a wristband during the TTE examination. The PPG features will be extracted from the signal and compared between participants with and without AS. The correlations between the echocardiographic parameters and the PPG characteristics will be analyzed.

**Conclusion:** The DETECT-REMOTE study aims to investigate the association between PPG signal characteristics and the presence, absence, or severity of AS. The results of this study may contribute to the development of a remote monitoring device for AS. A remote monitoring device could reduce the number of hospital visits and provide earlier detection of disease deterioration in patients with AS.

## 5.1 Introduction

Aortic valve stenosis (AS) is the second most prevalent valvular heart lesion with a poor prognosis once patients become symptomatic [1, 45]. Patients with AS undergo repeated transthoracic echocardiography (TTE) examinations to monitor disease progression. It remains challenging to anticipate to the unpredictable nature of AS deterioration [4]. A noninvasive tool to remotely monitor the progression of AS or detect severe AS could improve disease management and make the follow-up trajectory more efficient.

Photoplethysmography (PPG) is a noninvasive technique used to measure blood volume changes in the peripheral blood vessels. Various PPG signal characteristics have been demonstrated to correlate with different cardiovascular properties, such as blood pressure, stroke volume, and left ventricular ejection time [7, 33, 58]. Given that AS also affects these cardiovascular properties, the association between the PPG signal and AS was studied, as described in Chapter 4 [40]. This study compared the PPG signal pre- and post-transcatheter aortic valve implantation (TAVI) and revealed significant differences in the PPG signal before and after valve replacement. Although the findings are limited by the study setting in which data were recorded during surgery, the findings support our hypothesis on a potential impact of AS on the PPG signal recorded on the wrist. These promising results have sparked great interest in further investigating this association and overcoming the limitations of the study. Therefore, the DETECT-REMOTE study was set up.

The DETECT-REMOTE study will investigate the PPG signal during transthoracic echocardiograms (TTE). Acquisition of data during TTE prevents bias caused by surgical circumstances and provides the opportunity to investigate more subtle changes in aortic valve obstruction in native valves. The primary objective of this study is to investigate the wrist-derived PPG signal characteristics in relation to the presence or absence, and severity of AS in patients undergoing clinically indicated TTE. The secondary objective of this study is to investigate the PPG signal in relation to echocardiographic parameters related to left ventricular ejection,

aortic valve function, mitral valve regurgitation, or diastolic dysfunction. Furthermore, the data obtained during this study can be used to improve a circulatory arrest detection algorithm developed in the Radboudumc during the DETECT-1 study. The PPG data provide the possibility to further investigate false positive circulatory arrest alarms.

## 5.2 Study Design

### 5.2.1 Aim of the Study

The primary aim of the DETECT-REMOTE study is to investigate the PPG signal characteristics in relation to the presence or absence, and severity of AS.

### 5.2.2 Hypothesis

It is hypothesized that PPG signal characteristics differ in relation to the presence or absence of AS, and that patients with moderate or severe AS can be distinguished from those without AS based on differences in their PPG signal.

### 5.2.3 Overview of the study design

The DETECT-REMOTE study is an observational, prospective, single-center study to investigate the association between PPG signal characteristics and the presence, absence, or severity of AS. This will be investigated by comparing the PPG signals from patients with and without AS undergoing a clinically indicated TTE in the Radboudumc. Expected duration of the entire study is six months. For the individual participants, study duration is approximately one hour.

### 5.2.4 Eligibility criteria for the study

Eligible patients for the study are those who undergo a clinically indicated TTE at the outpatient clinic or the hospital ward of the Radboudumc cardiology department. All study participants are 18 years or older, fit the wristband, and undergo a clinically-indicated TTE at the Radboudumc for one of the following reasons: suspected or known AS, a bicuspid and stenotic aortic valve, or a non-stenotic native valve. Participants without AS will function as the reference group, and to ensure age-matched groups, at least half of this group should be 60 years or older. Patients will be excluded from the study in the case of known hemodynamically relevant subclavian artery stenosis, medical issues that interfere with wearing the wristband (e.g. skin

disorders), or if they are unwilling or unable to provide written informed consent.

### 5.2.5 Data collection and monitoring

PPG data will be collected with a CE-certified wristband, the Cardiowatch 287-2 (Corsano Health B.V.). The wristband will be placed on the right wrist, as patients must lie on their left side during TTE, which could displace the sensor if placed on the left wrist. For participants visiting the outpatient clinic, the wristband with PPG sensors will be worn during TTE. After completion of the TTE examination by the sonographer, the wristband will be removed and study participation is completed. For participants staying on the hospital ward, the wristband will be worn for one hour on the day of their TTE. After one hour, the wristband is removed and study participation is completed. Participants will not be asked to modify their behavior in any way during study participation. After removal of the wristband, there is no follow-up.

Echocardiographic data will be obtained by the sonographer according to standard clinical practice at Radboudumc. Data will be reported in the electronic patient record (EPR). The echocardiographic parameters used for this study will be retrieved from the EPR and stored in Castor Electronic Data Capture (EDC) (<https://www.castoredc.com/>). Castor EDC is also used as an electronic file form to store all data per participant. Baseline data will be obtained prior to wristband application by measuring the noninvasive blood pressure and the wrist circumference.

### 5.2.6 PPG Monitoring Device

The PPG data will be collected using the Cardiowatch 287-2 (Corsano Health B.V.). The Cardiowatch is an EU-MDR medically certified wristband designed to continuously monitor physiological data in home and healthcare settings. The PPG sensor contains light emitting diodes (LEDs) with green, red, and infrared light. Data are transmitted wirelessly with Bluetooth from the device to the Corsano application located on a

study phone. The application transfers the data to a health cloud where they are stored and made available for further analysis. The software complies with the privacy and security rules of the General Data Protection Regulation (GDPR) and the Health Insurance Portability and Accountability Act (HIPAA).

### 5.2.7 Study parameters

The primary study parameters are the PPG signal characteristics: systolic amplitude, area under the curve, pulse width at different heights, crest time, stiffness index, inflection point ratio, and heart rate (variability) measures. The PPG signal characteristics will be derived with the same method as described in Chapter 4. Secondary study parameters are echocardiographic parameters indicating: 1) left ventricular ejection; 2) aortic valve regurgitation; 3) mitral valve regurgitation; 3) diastolic dysfunction. Table 5 provides an overview of the echocardiographic parameters that will be used during the analysis. Other study parameters are demographic data (age and sex), medical history, a noninvasive blood pressure record, wrist circumference, skin type according to the Fitzpatrick scale (Appendix B.1), and hair density on the wrist.

### 5.2.8 PPG data analysis

Preprocessing of the PPG signal and feature extraction will be similar to the method described in Chapter 4. The PPG data will be filtered and high amplitude motion artifacts will be removed. Subsequently, 300 consecutive good-quality cardiac cycles will be detected with an automated algorithm. Time-domain features will be extracted per cardiac cycle, resulting in 300 values per patient. These values will be averaged, resulting in one value per patient. Frequency-domain features will be extracted from 300 consecutive peaks of sufficient quality, resulting in one value per patient. Preprocessing and feature extraction of the data will be performed using Python 3.8 (Python Software Foundation, Wilmington, United States)

## Second study

Table 5: Echocardiographic parameters that will be collected for this study including a brief description of the parameters. LVEF = left ventricular ejection fraction, LVET = left ventricular ejection time, AV = aortic valve, LVOT = left ventricular outflow tract, VTI = velocity time integral, PG = pressure gradient

Echocardiographic parameter	Description
Heart rhythm	Sinus rhythm or atrial fibrillation
Heart rate	Beats per minute
LVEF	Left ventricular ejection fraction
Right ventricular function	Poor, moderate, reasonable, or good
Diastolic dysfunction	Presence of diastolic dysfunction
Grade of diastolic dysfunction	Grade 1, grade 2, or grade 3
LVET	Left ventricular ejection time
Acceleration time over the AV	Time interval between the beginning of the systolic flow and its peak velocity
$V_{\max}$ over the AV	Maximum blood flow velocity over the AV during systole
LVOT diameter	Diameter of the left ventricular outflow tract
VTI LVOT	Velocity time integral over the LVOT representing the distance that blood travels during one heartbeat
VTI AV	Velocity time integral over the AV
Stroke volume	Calculated by the LVOT VTI multiplied with the cross sectional area of the LVOT
Aortic valve dimensionless index	Ratio between the VTI LVOT and the VTI AV
Aortic valve area	Area in $\text{cm}^2$
$\text{PG}_{\text{peak}}$	Maximum pressure gradient over the AV
$\text{PG}_{\text{mean}}$	Mean pressure gradient over the AV
The presence of valvular disease and its severity	Stenosis or regurgitation. Severity: mild, moderate, or severe

### 5.2.9 Statistical considerations

Statistical analysis will be performed using SPSS Statistics 27 (IBM, Armonk, USA). The PPG signal characteristics will be compared between the patient groups: presence and absence of AS. Baseline characteristics will be described per group. Continuous data will be evaluated for normal distribution and presented as means  $\pm$  standard deviation (SD) or medians with interquartile ranges, whichever is appropriate. The PPG signal characteristics of the group with AS will be compared with those of the group without AS using a Student's t-test or Mann-Whitney U test, whichever is appropriate.

Additionally, the PPG signal characteristics will be studied for each stage of AS. Comparisons between the four groups (absence of AS, mild, moderate, and severe AS) will be performed using the one-way ANOVA or Kruskal-Wallis test, whichever is appropriate. To determine whether there is a significant trend between the different stages of AS and the PPG signal characteristics, the Jonckheere-Terpstra test will be used. The correlations between

echocardiographic parameters that are on a continuous scale, blood pressure, and the PPG characteristics will be analyzed by determining Pearson's rho coefficient or Spearman's rho coefficient, whichever is appropriate.

PPG data will also be processed using the PPG-based algorithm developed in the DETECT-1 study. False positive circulatory arrest alarms will be studied by the number of participants with at least one false positive alarm and the number of alarms per hour (false positive rate). Subsequently, the data will be used to improve the circulatory arrest algorithm to reduce false positive alarms.

### 5.2.10 Sample size calculation

Sample size calculation was performed with the G\*Power 3.1 software package (Dusseldorf, Germany). The preliminary results of Chapter 4 were used to make reliable assumptions about the expected differences in PPG signal characteristics between patients with and without AS. The difference in crest time, which could be a promising feature for detecting AS according to Chapter 4, was

chosen for this analysis. The assumed mean change in crest time is from 0.245 to 0.275 (no AS vs. AS) with a pooled standard deviation of 0.045. To test this difference with a Wilcoxon signed-rank test with a p-value of 0.05 and a power of 90%, a total of 108 enrolled patients is required.

### 5.2.11 Study organization

This study is reviewed by the Medical Research Ethics Committee (MREC) and the institutional review board as a study that does not have to comply with the Medical Research Involving Human Subjects Act (WMO). This study is a non-WMO study, as there are no risks associated with wearing the wristband and the additional actions to participate in the study are minimal. The study protocol, the informed consent form, and the patient recruitment procedures have been approved by the institutional review board. This study is sponsored by the Radboudumc in Nijmegen, the Netherlands.

## 5.3 Discussion

The DETECT-REMOTE study is the first observational, prospective, single-center study to investigate the association between PPG signal characteristics and the presence, absence, or severity of AS. The results of this study can contribute to the development of a remote device to monitor disease progression of AS. An accurate at home monitoring device could lead to an earlier diagnosis of sudden disease deterioration and reduce the number of hospital visits due to more frequent follow-up at home.

Different studies have been published on the detection of AS with the use of cardiomechanical signals, such as the impedance cardiogram (ICG), seismocardiogram (SCG), and gyrocardiogram (GCG) [60-63]. These studies focused on the detection of AS and the classification of its severity with the use of a noninvasive and low-cost device. Shokouhmand et al. [60] demonstrated an impressive confidence in AS detection of 95.48 to 100.00% using their SCG- and GCG-based framework. Similarly, Chabchoub et al. [63] presented an ICG based method to detect all types of valve disease with an overall accuracy of 98.94%. However, these techniques require professional

application of the sensors, and therefore hospital visits are required, and daily use becomes impractical. Moreover, the complexity of their feature extraction methods and the use of machine learning or deep learning algorithms pose challenges in providing a physiological explanation for the findings of these studies.

### 5.3.1 Rationale for the intervention

To address these practical concerns, the DETECT-REMOTE study uses a wristband incorporating a PPG sensor, which offers continuous monitoring while ensuring comfort and ease of use. Furthermore, the extracted features in this study can be physiologically explained. The study described in Chapter 4 demonstrated that resolving aortic valve obstruction has a significant effect on the PPG signal characteristics. Based on these promising results, it is hypothesized that PPG could be used to distinguish between patients with and without AS.

In the literature there are limited examples of studies on the development of a wearable PPG sensor to detect AS. Simonyan et al. [10] demonstrated that patients with AS exhibit a higher percentage of low-frequency (%LF) and high-frequency (%HF) oscillations in the frequency spectrum of the PPG signals. Low-frequency oscillations are associated with sympathetic effects on peripheral vascular stiffness, while high-frequency oscillations are related to respiratory effects [10]. In patients with AS, the sympathetic influence on peripheral vascular stiffness increases, which could explain the increased LF%. Simonyan et al. [10] suggest that the elevated HF% may be attributed to an increased activity of the respiratory center in patients with AS. Additionally, there is an unpublished study registered on ClinicalTrials.gov. [64], employing a similar methodology with PPG recordings during echocardiography. The main outcome measure of this study is the association between the PPG waveforms and the recorded ejection fractions. Secondary outcomes are investigating the association between blood pressure and PPG and investigating the association between PPG and echocardiographic findings such as valvular heart disease, cardiomyopathies, and pericardial disease. Upon publication of the results

of this study, it would be valuable to compare these findings with those obtained from the DETECT-REMOTE study.

### 5.3.2 Rationale for the outcome measures

The same PPG signal characteristics as used in Chapter 4 will be used for this study, described in Table 2. In this way, the results of both studies can be compared. The amplitude-related features have been correlated with cardiac output in previous studies, and since cardiac output can be reduced with AS, these parameters could contribute to the detection of AS [7]. The pulse width has been correlated with the duration of a pulse wave to reach the arteriolar vessels [26]. This duration could be lengthened by increased systemic vascular resistance or by a longer left ventricular ejection time (LVET). The latter could be increased in patients with AS, and therefore pulse width is expected to be an indicator of AS progression [41]. The crest time, which is the time from the onset of the pulse wave to the systolic peak, is expected to be an indicator of AS progression, as demonstrated in Chapter 4. The crest time indicates the duration to reach the maximum blood volume in the peripheral vessels, which depends on peripheral resistance, blood pressure, and LVET.

Echocardiographic parameters will be used to obtain a comprehensive evaluation of the patient's heart function. Furthermore, the parameters can be used to identify and eliminate alternative factors that may contribute to differences in PPG signal characteristics observed between the groups.

### 5.3.3 Limitations

This study focuses on an interpatient comparison while a remote monitoring system assesses the PPG signal in an individual patient. This is an important difference that should be considered while interpreting the results.

Second, it is important to consider that external factors, such as contact between the skin and the sensor, can affect the amplitude of the PPG signal. This introduces a level of unreliability when comparing features related to amplitude, as they depend on factors other than solely physiological aspects.

Third, the results might be influenced by the age differences between the groups, since the occurrence of AS increases with age. Age has an impact on vascular stiffness and cardiovascular parameters, influencing the PPG wave morphology [9]. To mitigate this limitation, the control group should be matched with respect to age. Therefore, half of the reference group will be 60 years or older. Furthermore, a group of young patients with bicuspid stenotic valves will be included in the study to substantiate that the findings are due to AS rather than age.

Lastly, the presence of movement artifacts in the PPG signal could pose a limitation to the analysis. Although the Hilbert transform will be applied to filter out high-amplitude changes caused by movement, smaller changes in the signal morphology may still be present. These artifacts could influence the results. However, including movement may best reflect clinical reality during daily use of the wristband.

### 5.3.4 Current status

Currently, at the end of July 2023, 71 patients have been included in the study. Of these participants, nine have severe AS, nine have moderate AS, one has mild AS, four have bicuspid AS, and 48 do not suffer from AS. Recruitment started at the end of May 2023. Given the high percentage of patients who meet the inclusion and exclusion criteria and the high degree of willingness to participate in the study, the required number of participants is expected to be reached in time.

## Conclusion

The DETECT-REMOTE study is the first observational, prospective, single-center study to investigate the association between PPG signal characteristics and the presence, absence, or severity of AS. The results of this study may contribute to the development of a remote monitoring device for AS. A remote monitoring device could reduce the number of hospital visits and provide earlier detection of disease deterioration in patients with AS.

# Discussion

## 6.1 Summary of findings

To the best of our knowledge, this is the first study to investigate the association between wrist-derived PPG signal characteristics and the presence of AS. In this study, we developed an automated pulse wave selection algorithm that detects systolic peaks and their corresponding cardiac cycles from the PPG signal. Feature extraction made it possible to compare PPG signals between patients with and without AS. PPG signal characteristics differ markedly prior to and after valve implantation in patients with severe AS. The identified PPG differences are in line with the differences in aortic pressure after valve implantation observed by, which indicates the potential of PPG for noninvasive, remote, and more frequent AS monitoring [19].

In Chapter 4, the measurement of PPG during TAVI provided the opportunity to reveal the specific effects of aortic valve obstruction on the PPG signal due to isolated valve replacement. A significant increase was found after valve placement for the seven PPG features: heart rate, systolic amplitude, area under the curve, upstroke, downstroke, (b+e)/a ratio, and b/a ratio. A significant decrease was found after valve placement for the eight PPG features: crest time, e/a ratio, notch time, and the pulse width of the PPG signal at different heights. Parameters that differ significantly after valve placement hold potential as indicators of AS progression. However, the features and their specificity for AS progression should be further investigated under nonsurgical conditions.

In Chapter 5, the study design of the DETECT-REMOTE study was described. In this study, the wrist-derived PPG signal measured during TTE will be analyzed and compared between patients with and without AS. Measurement of the PPG signal during TTE will eliminate the effect that surgical conditions could have introduced on the results of the study during TAVI. Moreover, the DETECT-REMOTE study will focus on more subtle differences in aortic valve obstruction, since patients with mild, moderate and severe AS will be included.

## 6.2 Interpretation of findings

The results of the TAVI study suggest that a decrease in systolic amplitude, AUC, upstroke, downstroke, and an increase in crest time, notch time, and pulse width could be indicators of the presence or progression of AS. Physiological explanations for the observed changes in these PPG signal characteristics are an increased stroke volume and a decreased LVET due to resolving the aortic valve obstruction [19]. However, it is essential to consider that these parameters are also influenced by various other hemodynamic factors and physical conditions, making it challenging to solely rely on these features for AS detection. For this reason, these features may not be directly used for AS detection, but they could serve as indicators of disease progression. If these features are used to monitor disease progression it is important to obtain full understanding of the course of these hemodynamic parameters with the different stages of AS. The course of LVET can be understood by Equation 11 which describes the relation between the LVET and AVA [65]:

$$(6) \quad LVET = k * \frac{SV}{\sqrt{PG}} * \frac{1}{AVA}$$

In this equation, LVET is the left ventricular ejection time, k is a constant ( $\text{cm/s}^2$ ), SV is the stroke volume, PG is the mean aortic pressure gradient and AVA is the aortic valve area. Notably, the LVET is not linearly dependent on the AVA and the LVET is influenced by the severity of AS and overall ventricular function. Disease progression of AS is characterized by a decreased AVA, leading to an initial compensatory increase in LVET to preserve cardiac output. As AS becomes more severe, the LVET may decrease with deterioration of ventricular function. However, when AS reaches an exceedingly severe stage ( $\text{AVA} < 1 \text{ cm}^2$ ), the LVET will increase progressively, as the outcome is multiplied by the reciprocal of the AVA. This non-linear and unpredictable course of the LVET during disease progression makes it challenging to use this parameter as a definitive marker of AS progression. For a comprehensive evaluation of disease progression, other clinical and diagnostic parameters should be considered as well. The combination of multiple indicators will provide a more accurate assessment of AS severity and disease progression.

Although significant differences in multiple PPG signal characteristics have been found after valve placement, a considerable degree of overlap was observed in the interquartile ranges (IQRs). This observation underscores the complexity of establishing distinct patient groups based solely on PPG signal differences within an intrapatient analysis. During the DETECT-REMOTE study an interpatient analysis will be performed and it will be interesting to explore whether patients without AS and those with varying degrees of AS severity (mild, moderate, or severe) exhibit features that could potentially be used for AS stratification. For monitoring AS progression, it is not necessary to create distinct groups, as the PPG signal characteristics of an individual patient will be compared over time. To investigate the course of the PPG signal characteristics with AS progression, it is recommended to perform a longitudinal study.

### 6.3 Clinical implications

A review article on the status and future perspectives of patient screening states that the first challenge in mitigating the impact of AS on society is increasing timely diagnoses of AS [3]. The development of a remote monitoring device that is noninvasive and easy to use could contribute to the solution to this major challenge. The convenience of wearable PPG sensors in these contexts lies in their potential to replace or support invasive and time-consuming clinical tests [66]. These traditional tests, such as TTE, are typically conducted at specific intervals and often require the presence of a clinical expert and expensive equipment. In contrast, PPG-based methods offer the advantage of remote monitoring without direct patient involvement and minimal training. It is important to note that PPG-based approaches may not fully replace clinical tests due to their often inferior performance [66]. Therefore, the primary role of PPG-based approaches is likely to be centered around the early detection of cardiovascular disease and constant measurement of risk factors. These measurements could then prompt further clinical evaluation.

If the results of the DETECT-REMOTE study support the findings of the study described in Chapter 4, the potential of PPG for AS monitoring would be reinforced. Additionally, any relevant correlations discovered between echocardiographic parameters and PPG signal characteristics could potentially extend the use of remote monitoring tools to other cardiac conditions. An ongoing trial by Tulane University (New Orleans, United States) [64] focuses on the association between the LVEF and the PPG signal in the general population. The DETECT-REMOTE study acquires PPG data from patients with a wide range of LVEF values and, therefore, it would be valuable to investigate this association and compare the results with the ongoing trial. A remote and noninvasive tool to monitor the LVEF could have major clinical implications since this is the main parameter for the assessment of systolic function. This could improve disease management of patients with heart failure as early detection of disease deterioration could reduce hospitalization or mortality.

In the literature, few studies have been published on alternative monitoring techniques for AS. Although the studies by Chabchoub [63] and Shokouhmand [60] et al. show high performance in detecting AS with cardiomechanical sensors, these sensors are not yet integrated into clinical practice. The limitations of these sensors are the need for professional application and impracticality for daily use. The use of a wristband incorporating a PPG sensor could overcome these limitations since this device is practical for daily use. Monitoring of AS does not have to be continuously, and one or two measuring moments a month would already be beneficial compared to a TTE once a year or every two years. It is advised to perform measurements during sleep to reduce the influence of motion and obtain comparable measurements. Future research will need to determine whether this is indeed the most optimal measurement moment and how sleep patterns might influence the PPG signal. Moreover, before clinical implementation is possible, numerous considerations have to be addressed. Questions pertaining patient compliance, real-time feedback on deterioration or AS detection, the responsibility for data analysis and interpretation, accuracy of the sensor, cost-effectiveness, and integration into the patient's care path need thorough investigation.

### 6.4 Recommendations

Based on the findings presented in this study, several recommendations can be made to further enhance the understanding of the association between the PPG signal and AS. First, the TTE study should be performed and the results should be compared with the results of the TAVI study. The presence of overlapping IQRs before and after valve placement during the TAVI study, shows that it is not possible to categorize patients based on individual features. Therefore, it is recommended to perform a multivariable analysis during the TTE study and develop a detection model for the absence, presence, or stage of AS based on multiple features.

Secondly, it is recommended to incorporate additional features into future investigations, such as the perfusion index. The perfusion index is the ratio between the amplitude of the AC and DC component of the PPG signal. Since external conditions will affect the amplitudes in a similar way, the ratio is a more reliable parameter than the systolic amplitude of the AC component alone [67]. In the TAVI study, the external conditions did not change and intrapatient comparisons were made. During the TTE study, interpatient comparisons will be made and therefore the perfusion index would be recommended to use in this study. Another feature that could be interesting to investigate is the pulse transit time. The pulse transit time is the time interval from the ECG R-peak to the onset of the synchronized PPG signal. This feature is influenced by arterial stiffness, but could also be affected by the LVET. The Cardiowatch also has the ability to measure the ECG signal, and this could thus be incorporated in the analysis.

In addition, it is recommended to use the data obtained during the DETECT-REMOTE study to investigate the prediction of echocardiographic parameters using the PPG signal. A recently published abstract showed that it was feasible to use wrist-derived PPG for real-time monitoring of the LVOT VTI and the LVEF, with a precision of 4.02 cm and 0.77% respectively [68]. The DETECT-REMOTE study will include a larger and more diverse study population, providing a unique opportunity to delve deeper into investigating the prediction of echocardiographic parameters utilizing the PPG signal. This could potentially improve the monitoring of AS and other cardiac diseases, such as heart failure.

Finally, the potential of PPG for monitoring AS should be further investigated during longitudinal studies. Such studies, conducted over an extended period of time, would allow the observation of changes and trends in the characteristics of the PPG signal among AS patients. This longitudinal approach has the potential to reveal dynamic patterns and provide valuable insights into the progression of the disease, contributing to better informed treatment decisions.

## Conclusion

The TAVI study showed promising results on the analysis of the wrist-derived PPG signal in patients with AS. PPG signal characteristics markedly differ between before and after valve placement in patients with severe AS. This indicates the potential of these features for remote monitoring of AS. This warrants further investigation as to whether wrist-derived PPG can be used to remotely monitor AS progression.

To further investigate the association between AS and PPG, the DETECT-REMOTE study was set up. This study focuses on measuring the PPG signal during TTE to obtain an interpatient comparison in nonsurgical settings. If the results of this study support the findings of the TAVI study, this could have a major impact on the development of a remote monitoring device for AS. To advance our understanding in this field, more research is imperative. First, the results of the DETECT-REMOTE study should be analyzed and compared with the TAVI study. Furthermore, longitudinal studies focusing on obtaining intrapatient data from individuals with AS would be valuable in exploring the long-term dynamics and progression of AS.

In conclusion, although the TAVI study shows promising results, further research into the potential of PPG in monitoring AS is warranted. Comparison of the results of the TAVI study and the DETECT-REMOTE study will contribute to a better understanding of the wrist-derived PPG signal in the context of AS and its potential clinical applications.

## Contribution of the author

In this section I will shortly describe my contribution to the studies described in this thesis. For the first study, the TAVI study, I participated in the patient inclusions from October 2022 to May 2023. My contribution consisted of screening patients, explaining the study procedure to the patients at the cardiology ward, obtaining written informed consent, and starting the measurements during the TAVI procedure on the cardiac catheterization room. This was a sub-analysis of the DETECT-1 study and I supported the PhD student responsible for this study, but I did not include all patients myself. For the DETECT-REMOTE study, I wrote the study protocol and the informed consent forms which have been approved by the METC and the institutional review board as a non-WMO study. The initiation of the DETECT-REMOTE study was also my responsibility, which consisted of drawing up the correct documents (worklist, identification log, screening log etc.), and informing the sonographers and other involved colleagues about the study. For this study, I included all 71 patients myself.

# References

1. Osnabrugge, R.L.J., et al., *Aortic Stenosis in the Elderly: Disease Prevalence and Number of Candidates for Transcatheter Aortic Valve Replacement: A Meta-Analysis and Modeling Study*. Journal of the American College of Cardiology, 2013. **62**(11): p. 1002-1012.
2. Vahanian, A., et al., *2021 ESC/EACTS Guidelines for the management of valvular heart disease: developed by the Task Force for the management of valvular heart disease of the European Society of Cardiology (ESC) and the European Association for Cardio-Thoracic Surgery (EACTS)*. European heart journal, 2022. **43**(7): p. 561-632.
3. Thoenes, M., et al., *Patient screening for early detection of aortic stenosis (AS)-review of current practice and future perspectives*. J Thorac Dis, 2018. **10**(9): p. 5584-5594.
4. Shah, S.M., et al., *Pathophysiology, emerging techniques for the assessment and novel treatment of aortic stenosis*. Open Heart, 2023. **10**(1).
5. BV, C.H. *Brochure Corsano 287-1*. 2022.
6. Reguig, F.B. *Photoplethysmogram signal analysis for detecting vital physiological parameters: An evaluating study*. in *2016 International Symposium on Signal, Image, Video and Communications (ISIVC)*. 2016. IEEE.
7. Lee, Q.Y., et al., *Estimation of cardiac output and systemic vascular resistance using a multivariate regression model with features selected from the finger photoplethysmogram and routine cardiovascular measurements*. BioMedical Engineering OnLine, 2013. **12**(1): p. 1-15.
8. Wang, L., et al. *Noninvasive cardiac output estimation using a novel photoplethysmogram index*. in *2009 annual international conference of the IEEE engineering in medicine and biology society*. 2009. IEEE.
9. Charlton, P.H., et al., *Assessing hemodynamics from the photoplethysmogram to gain insights into vascular age: A review from VascAgeNet*. American Journal of Physiology-Heart and Circulatory Physiology, 2022. **322**(4): p. H493-H522.
10. Simonyan, M., et al., *Features of Spectral Estimates of the Photoplethysmographic Waveform Variability in Patients with Aortic Stenosis*. Biomedical and Pharmacology Journal, 2022. **15**(3): p. 1239-1244.
11. Joseph, J., et al., *Aortic stenosis: pathophysiology, diagnosis, and therapy*. The American journal of medicine, 2017. **130**(3): p. 253-263.
12. Moore, K.L., A.M.R. Agur, and A.F. Dalley, *Essential Clinical Anatomy*. 2015: Wolters Kluwer Health.
13. Crawford, P.T. and B. Bordoni, *Anatomy, Thorax, Aortic Valve*, in *StatPearls [Internet]*. 2021, StatPearls Publishing.
14. Sverdlov, A.L., et al., *Pathogenesis of aortic stenosis: not just a matter of wear and tear*. American journal of cardiovascular disease, 2011. **1**(2): p. 185.
15. Kong, W.K., et al., *Sex differences in bicuspid aortic valve disease*. Progress in Cardiovascular Diseases, 2020. **63**(4): p. 452-456.
16. Selle, A., et al., *Impact of rapid ventricular pacing during TAVI on microvascular tissue perfusion*. Clinical Research in Cardiology, 2014. **103**(11): p. 902-911.
17. Medtronic, *Brochure Evolut PRO+ Transcatheter Aortic Valve System*. 2023: medtronic.eu.
18. Perriello, B. *TAVI: Strong results for heart valves from Edwards Lifesciences, Medtronic*. 2015; Available from: <https://www.massdevice.com/tavi-strong-results-heart-valves-edwards-lifesciences-medtronic/>.
19. Pagoulatou, S., et al., *Acute effects of transcatheter aortic valve replacement on the ventricular-aortic interaction*. American Journal of Physiology-Heart and Circulatory Physiology, 2020. **319**(6): p. H1451-H1458.

## References

---

20. Perlman, G.Y., et al., *Post-procedural hypertension following transcatheter aortic valve implantation: incidence and clinical significance*. JACC Cardiovasc Interv, 2013. **6**(5): p. 472-8.
21. Yotti, R., et al., *Systemic Vascular Load in Calcific Degenerative Aortic Valve Stenosis*. Journal of the American College of Cardiology, 2015. **65**(5): p. 423-433.
22. Park, J., et al., *Photoplethysmogram Analysis and Applications: An Integrative Review*. Frontiers in Physiology, 2022. **12**.
23. Alian, A.A. and K.H. Shelley, *Photoplethysmography*. Best Practice & Research Clinical Anaesthesiology, 2014. **28**(4): p. 395-406.
24. Kyriacou, P.A. and J. Allen, *Photoplethysmography: Technology, Signal Analysis and Applications*. 2021: Elsevier Science.
25. Elgendi, M., *On the analysis of fingertip photoplethysmogram signals*. Current cardiology reviews, 2012. **8**(1): p. 14-25.
26. Awad, A.A., et al., *The relationship between the photoplethysmographic waveform and systemic vascular resistance*. Journal of Clinical Monitoring and Computing, 2007. **21**(6): p. 365-372.
27. Einarsen, E., et al., *Higher Acceleration/Ejection Time Ratio Predicts Impaired Outcome in Aortic Valve Stenosis*. Circulation: Cardiovascular Imaging, 2021. **14**(1).
28. Finnegan, E., et al., *Features from the photoplethysmogram and the electrocardiogram for estimating changes in blood pressure*. Scientific Reports, 2023. **13**(1): p. 986.
29. Maeder, M.T., et al., *Systemic blood pressure in severe aortic stenosis: Haemodynamic correlates and long-term prognostic impact*. ESC Heart Failure, 2023. **10**(1): p. 274-283.
30. Alty, S.R., et al., *Predicting arterial stiffness from the digital volume pulse waveform*. IEEE Transactions on Biomedical Engineering, 2007. **54**(12): p. 2268-2275.
31. Djeldjli, D., et al. *Imaging Photoplethysmography: Signal Waveform Analysis*. in *2019 10th IEEE International Conference on Intelligent Data Acquisition and Advanced Computing Systems: Technology and Applications (IDAACS)*. 2019.
32. Blok, S., et al., *The accuracy of heartbeat detection using photoplethysmography technology in cardiac patients*. Journal of Electrocardiology, 2021. **67**: p. 148-157.
33. Chowdhury, M.H., et al., *Estimating blood pressure from the photoplethysmogram signal and demographic features using machine learning techniques*. Sensors, 2020. **20**(11): p. 3127.
34. Takazawa, K., et al., *Assessment of Vasoactive Agents and Vascular Aging by the Second Derivative of Photoplethysmogram Waveform*. Hypertension, 1998. **32**(2): p. 365-370.
35. Garbi, M., *The general principles of echocardiography*, in *The EAE Textbook of Echocardiography*. 2011, Oxford University Press, New York. p. 1-13.
36. Ring, L., et al., *Echocardiographic assessment of aortic stenosis: a practical guideline from the British Society of Echocardiography*. Echo Res Pract, 2021. **8**(1): p. G19-g59.
37. Clavel, M.A., et al., *Aortic valve area calculation in aortic stenosis by CT and Doppler echocardiography*. JACC Cardiovasc Imaging, 2015. **8**(3): p. 248-257.
38. Baumgartner, H., et al., *Echocardiographic assessment of valve stenosis: EAE/ASE recommendations for clinical practice*. J Am Soc Echocardiogr, 2009. **22**(1): p. 1-23; quiz 101-2.
39. Carabello, B.A. and W.J. Paulus, *Aortic stenosis*. The lancet, 2009. **373**(9667): p. 956-966.
40. Carabello, B.A., *How Does the Heart Respond to Aortic Stenosis*. Circulation: Cardiovascular Imaging, 2013. **6**(6): p. 858-860.
41. Pestelli, G., et al., *Value of Left Ventricular Indexed Ejection Time to Characterize the Severity of Aortic Stenosis*. Journal of Clinical Medicine, 2022. **11**(7): p. 1877.
42. Kamimura, D., et al., *Delayed Time to Peak Velocity Is Useful for Detecting Severe Aortic Stenosis*. Journal of the American Heart Association, 2016. **5**(10): p. e003907.
43. Altes, A., et al., *Dimensionless Index in Patients With Low-Gradient Severe Aortic Stenosis and Preserved Ejection Fraction*. Circulation: Cardiovascular Imaging, 2020. **13**(10): p. e010925.

44. Rusinaru, D., et al., *Relation of Dimensionless Index to Long-Term Outcome in Aortic Stenosis With Preserved LVEF*. JACC: Cardiovascular Imaging, 2015. **8**(7): p. 766-775.

45. Clark, M.A., et al., *Five-year clinical and economic outcomes among patients with medically managed severe aortic stenosis: results from a Medicare claims analysis*. Circulation: Cardiovascular Quality and Outcomes, 2012. **5**(5): p. 697-704.

46. Allen, J., *Photoplethysmography and its application in clinical physiological measurement*. Physiological measurement, 2007. **28**(3): p. R1.

47. CorsanoHealth. *The Cardiowatch Bracelet*. 2023 [cited 2023 31-05-2023]; Available from: <https://corsano.com/products/bracelet-2/>.

48. Pereira, T., et al., *Photoplethysmography based atrial fibrillation detection: a review*. npj Digital Medicine, 2020. **3**(1): p. 3.

49. Fischer, C., et al., *An Algorithm for Real-Time Pulse Waveform Segmentation and Artifact Detection in Photoplethysmograms*. IEEE Journal of Biomedical and Health Informatics, 2017. **21**(2): p. 372-381.

50. Liu, S.H., et al., *Evaluating Quality of Photoplethysmographic Signal on Wearable Forehead Pulse Oximeter With Supervised Classification Approaches*. IEEE Access, 2020. **8**: p. 185121-185135.

51. Elgendi, M., et al., *Systolic Peak Detection in Acceleration Photoplethysmograms Measured from Emergency Responders in Tropical Conditions*. PLOS ONE, 2013. **8**(10): p. e76585.

52. Lewis, R.P., et al., *A critical review of the systolic time intervals*. Circulation, 1977. **56**(2): p. 146-158.

53. Sarnari, R., et al., *Doppler Assessment of the Ratio of the Systolic to Diastolic Duration in Normal Children: Relation to Heart Rate, Age and Body Surface Area*. Journal of the American Society of Echocardiography, 2009. **22**(8): p. 928-932.

54. Xiong, L., et al., *Multi-center pragmatic studies evaluating the time indicator of cardiac perfusion reserve*. Journal of Biomedical Science and Engineering, 2013. **6**.

55. Lin, C.P., et al., *Left Ventricular Systolic Function is Sensitive to Cycle-Length Irregularity in Patients with Atrial Fibrillation and Systolic Dysfunction*. Acta Cardiologica Sinica, 2012. **28**: p. 103-110.

56. Millasseau, S.C., et al., *Contour analysis of the photoplethysmographic pulse measured at the finger*. Journal of Hypertension, 2006. **24**(8).

57. Jung, H., et al., *Performance evaluation of a wrist-worn reflectance pulse oximeter during sleep*. Sleep Health, 2022. **8**(5): p. 420-428.

58. Chan, G.S., et al., *Automatic detection of left ventricular ejection time from a finger photoplethysmographic pulse oximetry waveform: comparison with Doppler aortic measurement*. Physiol Meas, 2007. **28**(4): p. 439-52.

59. Afshar, A.H., L. Pourafkari, and N.D. Nader, *Periprocedural considerations of transcatheter aortic valve implantation for anesthesiologists*. J Cardiovasc Thorac Res, 2016. **8**(2): p. 49-55.

60. Shokouhmand, A., et al., *Efficient detection of aortic stenosis using morphological characteristics of cardiomechanical signals and heart rate variability parameters*. Scientific Reports, 2021. **11**(1): p. 23817.

61. Yang, C., et al., *Classification of aortic stenosis using conventional machine learning and deep learning methods based on multi-dimensional cardio-mechanical signals*. Scientific Reports, 2020. **10**(1): p. 17521.

62. Johnson, E.M., et al., *Abstract 9903: Artificial Intelligence Driven Wearable 2-minute Seismocardiography Test for Detection of Aortic Valve Stenosis Severity*. Circulation, 2022. **146**(Suppl\_1): p. A9903-A9903.

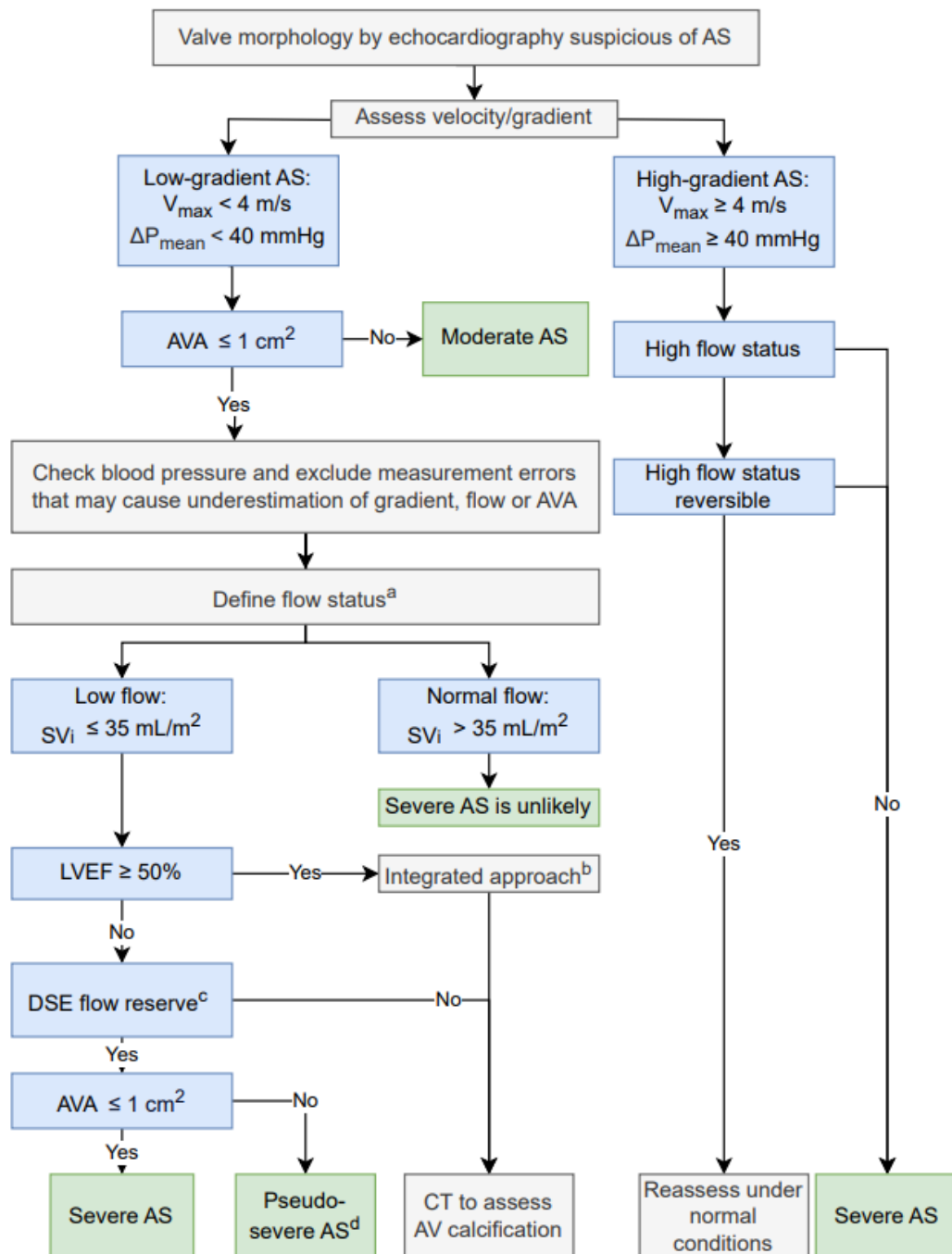
63. Chabchoub, S., S. Mansouri, and R. Ben Salah, *Detection of valvular heart diseases using impedance cardiography ICG*. Biocybernetics and Biomedical Engineering, 2018. **38**(2): p. 251-261.

## References

---

64. Marrouche, N. *PPG to Predict Ejection Fraction and Other Echographic Data in the General Population*. 2021; Available from: <https://clinicaltrials.gov/study/NCT04843371>.
65. Kligfield, P., et al., *Duration of ejection in aortic stenosis: Effect of stroke volume and pressure gradient*. Journal of the American College of Cardiology, 1984. **3**(1): p. 157-161.
66. Charlton, P.H., et al., *Wearable Photoplethysmography for Cardiovascular Monitoring*. Proc IEEE Inst Electr Electron Eng, 2022. **110**(3): p. 355-381.
67. Coutrot, M., et al., *Perfusion index: Physical principles, physiological meanings and clinical implications in anaesthesia and critical care*. Anaesthesia Critical Care & Pain Medicine, 2021. **40**(6): p. 100964.
68. Krishnan, S., et al., *ESTIMATION OF ECHOCARDIOGRAPHIC PARAMETERS OF SYSTOLIC FUNCTION FROM ANALYSIS OF PHOTOPLETHYSMOGRAPHY BASED ARTERIAL PULSE WAVE USING AUTOMATED FEATURE SELECTION*. Journal of the American College of Cardiology, 2023. **81**(8\_Supplement): p. 2207-2207.

# Appendix A Figures



Appendix A.1: Flowchart of the integrated assessment of aortic stenosis defined by the European Society of Cardiology. This figure is modified from [2]. AS = aortic stenosis; AV = aortic valve; AVA = aortic valve area; CT = computed tomography;

$\Delta P_{\text{mean}}$  = mean pressure gradient; DSE = dobutamine stress echocardiography; LV = left ventricle; LVEF = left ventricular ejection fraction;  $SV_i$  = stroke volume index;  $v_{\text{max}}$  = peak transvalvular velocity. a) High flow may be reversible in patients with several conditions such as anaemia, hyperthyroidism, or arterio-venous fistulae. b) Consider also: typical symptoms (without other explanation), LV hypertrophy or reduced LV longitudinal function. c) DSE flow reserve ≥ 20% increase in stroke volume in response to low-dose dobutamine. d) pseudo-severe AS is an AVA ≥ 1 cm<sup>2</sup> with an increased flow.

# Appendix B Tables

Appendix B.1: Descriptive statistics of two groups: participants that were excluded from the TAVI study because their data quality was insufficient and participants that were included in the TAVI study.

Characteristic	Excluded participants	Included participants
Age, years ( $\pm SD$ )	78 ( $\pm 7.3$ )	80 ( $\pm 6.3$ )
Female gender, no. (%)	17 (45.9%)	88 (56.4%)
BMI, kg/m <sup>2</sup> (IQR)	27.7 (23.9 - 32.2)	26.9 (24.0 - 29.4)
LVEF prior to TAVR, % (IQR)	50 (43.5 - 58)	55 (45 - 60)
Wrist circumference, cm (IQR)	17.5 (16 - 18.4)	17 (16-18)
Skin type on Fitzpatrick scale*	1	2 (5.4%)
	2	22 (59.5%)
	3	13 (35.1%)
	4	0 (0%)
	5	0 (0%)
	6	0 (0%)
	Nil	13 (35.1%)
	Sparse	14 (37.8%)
Hair density**	Moderate	9 (24.3%)
	Dense	0 (0%)
		2 (5.4%)
		15 (9.6%)
History of peripheral artery disease, no. (%)	17 (45.9%)	82 (52.6%)
History of hypertension, no. (%)	13 (35.1%)	44 (28.2%)
History of diabetes, no. (%)		

\* Fitzpatrick scale



\*\* Hair density scale



Appendix B.2: Median and interquartile ranges (IQR) of the wrist-derived PPG signal characteristics obtained during TTE for participants without a cardiac history and participants with moderate or severe AS. The p-value was obtained using a Mann-Whitney U test.

		No cardiac history (n=10)		Moderate or severe AS (n=6)	p-value
		Median	IQR	Median	IQR
<i>PPG features derived from the infrared PPG signal</i>					
Systolic amplitude	52.189	30.977 - 76.044		103.279	57.831 - 128.741
Syst. amp. gain	27.84	24.725 - 61.587		56.594	28.915 - 113.878
Syst. Amp. LED	4.017	2.057 - 5.283		5.295	3.922 - 7.946
AUC/R-R	58.230	37.067 - 97.919		119.553	66.802 - 140.616
B/A ratio	-0.030	-0.039 - -0.018		-0.023	-0.035 - -0.020
E/A ratio	0.022	0.015 - 0.038		0.017	0.014 - 0.027
BE/A ratio	-0.053	-0.080 - -0.033		-0.039	-0.062 - -0.035
Augmentation index	0.449	0.157 - 0.668		0.371	0.139 - 0.539
Stiffness index	780.649	756.431 - 877.315		747.615	368.014 - 829.602
IPA	2.359	1.376 - 2.797		2.13	1.267 - 5.579
Upstroke / R-R	44.892	351.888 - 808.715		915.557	616.384 - 1252.854
Downstroke / R-R	196.422	160.199 - 287.042		398.019	264.458 - 527.46
PW 50% / R-R	0.536	0.524 - 0.556		0.513	0.499 - 0.540
PW 60% / R-R	0.443	0.418 - 0.474		0.437	0.406 - 0.465
PW 70% / R-R	0.351	0.301 - 0.397		0.353	0.313 - 0.386
PW 80% / R-R	0.234	0.221 - 0.301		0.261	0.233 - 0.288
PW 90% / R-R	0.151	0.136 - 0.187		0.166	0.156 - 0.177
Notch time	0.455	0.433 - 0.467		0.454	0.420 - 0.500
<i>PPG signal characteristics derived from the green PPG signal</i>					
Beats per minute	64.419	62.679 - 67.038		76.849	68.347 - 80.438
STD of R-R interval	46.047	37.047 - 102.343		44.629	26.885 - 74.562
Low frequency %	19.037	9.759 - 35.334		14.014	12.601 - 19.679
High frequency %	32.994	16.962 - 64.553		63.444	11.085 - 73.146
Crest time / R-R	0.324	0.302 - 0.367		0.352	0.306 - 0.404
					0.937

Appendix A.3: Mean and standard deviations (SD) of the echocardiographic parameters for the participants without AS, participants with moderate AS, and participants with severe AS.

	No AS		Moderate AS (n=2)		Severe AS (n=4)		
	Mean	SD	N	Mean	SD	Mean	SD
LVEF	54.91	7.66	22.00	59.95	8.56	52.08	17.27
Vmax AV	1.44	0.37	20.00	2.59	0.45	3.90	0.60
LVOT diameter	21.32	2.47	11.00	19.75	1.77	22.25	2.75
VTI LVOT	22.77	4.92	22.00	18.50	3.54	20.75	5.68
Stroke volume	82.37	25.22	11.00	57.66	5.90	71.84	14.38
VTI AV	35.45	10.88	11.00	62.00	12.73	81.00	12.88
DI	0.72	0.16	11.00	0.32	0.12	0.25	0.03
AVA	2.69	0.94	9.00	0.94	0.20	0.98	0.14
AV PGmean	5.92	3.80	12.00	15.00	5.66	36.25	12.69
AV PGpeak	10.00	5.79	22.00	27.50	9.19	62.25	17.78